IAEA TECDOC SERIES

Therapeutic Radiopharmaceuticals Labelled with Copper-67, Rhenium-186 and Scandium-47

IAEA

International Atomic Energy Agency

THERAPEUTIC RADIOPHARMACEUTICALS LABELLED WITH COPPER-67, RHENIUM-186 AND SCANDIUM-47

The following States are Members of the International Atomic Energy Agency:

AFGHANISTAN	GEORGIA	OMAN
ALBANIA	GERMANY	PAKISTAN
ALGERIA	GHANA	PALAU
ANGOLA	GREECE	PANAMA
ANTIGUA AND BARBUDA	GRENADA	PAPUA NEW GUINEA
ARGENTINA	GUATEMALA	PARAGUAY
ARMENIA	GUYANA	PERU
AUSTRALIA	HAITI	PHILIPPINES
AUSTRIA	HOLY SEE	POLAND
AZERBAIJAN	HONDURAS	PORTUGAL
BAHAMAS	HUNGARY	QATAR
BAHRAIN	ICELAND	REPUBLIC OF MOLDOVA
BANGLADESH	INDIA	ROMANIA
BARBADOS	INDONESIA	RUSSIAN FEDERATION
BELARUS	IRAN, ISLAMIC REPUBLIC OF	RWANDA
BELGIUM	IRAQ	SAINT LUCIA
BELIZE	IRELAND	SAINT VINCENT AND
BENIN	ISRAEL	THE GRENADINES
BOLIVIA, PLURINATIONAL	ITALY	SAN MARINO
STATE OF	JAMAICA	SAUDI ARABIA
BOSNIA AND HERZEGOVINA	JAPAN	SENEGAL
BOTSWANA	JORDAN	SERBIA
BRAZIL	KAZAKHSTAN	SEYCHELLES
BRUNEI DARUSSALAM	KENYA	SIERRA LEONE
BULGARIA	KOREA, REPUBLIC OF	SINGAPORE
BURKINA FASO	KUWAIT	SLOVAKIA
BURUNDI	KYRGYZSTAN	SLOVENIA
CAMBODIA	LAO PEOPLE'S DEMOCRATIC	SOUTH AFRICA
CAMEROON	REPUBLIC	SPAIN
CANADA	LATVIA	SRI LANKA
CENTRAL AFRICAN	LEBANON	SUDAN
REPUBLIC	LESOTHO	SWEDEN
CHAD	LIBERIA	SWITZERLAND
CHILE	LIBYA	SYRIAN ARAB REPUBLIC
CHINA	LIECHTENSTEIN	TAJIKISTAN
COLOMBIA	LITHUANIA	THAILAND
COMOROS	LUXEMBOURG	TOGO
CONGO	MADAGASCAR	TRINIDAD AND TOBAGO
COSTA RICA	MALAWI	TUNISIA
CÔTE D'IVOIRE	MALAYSIA	TURKEY
CROATIA	MALI	TURKMENISTAN
CUBA	MALTA	UGANDA
CYPRUS	MARSHALL ISLANDS	UKRAINE
CZECH REPUBLIC	MAURITANIA	UNITED ARAB EMIRATES
DEMOCRATIC REPUBLIC	MAURITIUS	UNITED KINGDOM OF
OF THE CONGO	MEXICO	GREAT BRITAIN AND
DENMARK	MONACO	NORTHERN IRELAND
DJIBOUTI	MONGOLIA	UNITED REPUBLIC
DOMINICA	MONTENEGRO	OF TANZANIA
DOMINICAN REPUBLIC	MOROCCO	UNITED STATES OF AMERICA
ECUADOR	MOZAMBIQUE	URUGUAY
EGYPT	MYANMAR	UZBEKISTAN
EL SALVADOR	NAMIBIA	VANUATU
ERITREA	NEPAL	VENEZUELA, BOLIVARIAN
ESTONIA	NETHERLANDS	REPUBLIC OF
ESWATINI	NEW ZEALAND	VIET NAM
ETHIOPIA	NICARAGUA	YEMEN
FIJI	NIGER	ZAMBIA
FINLAND	NIGERIA	ZIMBABWE
FRANCE	NORTH MACEDONIA	
GABON	NORWAY	

The Agency's Statute was approved on 23 October 1956 by the Conference on the Statute of the IAEA held at United Nations Headquarters, New York; it entered into force on 29 July 1957. The Headquarters of the Agency are situated in Vienna. Its principal objective is "to accelerate and enlarge the contribution of atomic energy to peace, health and prosperity throughout the world".

THERAPEUTIC RADIOPHARMACEUTICALS LABELLED WITH COPPER-67, RHENIUM-186 AND SCANDIUM-47

COPYRIGHT NOTICE

FOREWORD

Theranostic radiopharmaceuticals have shown tremendous promise in the past decade for the treatment and diagnosis of human diseases via nuclear medicine procedures. The idea of using a pair of radionuclides, or different radioactivities of the same radionuclide, to both detect and treat cancerous cells was initiated at the beginning of radiopharmacy with the introduction of ^{131}I in the 1950s. However, the need for stable, ready to use and commercially available radiopharmaceuticals led to the development of metal based radiopharmaceuticals with therapeutic and diagnostic capabilities, including ^{68}Ga and ^{177}Lu in the 2000s.

With the development of diverse carrier molecules of different molecular sizes and biological half-lives for targeting human diseases at the molecular level, and in response to the global personalized medicine movement, it was considered necessary to develop additional theranostic radionuclides with varying half-lives, decay characteristics and chelation chemistry for both theranostic activity and dosimetric aspects.

To address this need, and in response to requests from Member States and professional societies, the IAEA initiated the Therapeutic Radiopharmaceuticals Labelled with New Emerging Radionuclides (^{67}Cu, ^{186}Re, ^{47}Sc) coordinated research project. The project, carried out from 2016 to 2020, focused in particular on the production, quality control and radiopharmaceutical aspects of three selected radionuclides: ^{67}Cu, ^{186}Re and ^{47}Sc.

The present publication was compiled using the results of this CRP as well as inputs from experts in the field. It contains separate sections for each radionuclide on nuclear data, targetry, irradiation, chemical separation, quality control and sample radiopharmaceutical production.

The IAEA wishes to thank the participating experts for their contributions, in particular to S.E. Lapi (United States of America) for compiling and editing the contributed material, and J. Vera Araujo (Bolivarian Republic of Venezuela) for her editorial support. The IAEA officer responsible for this publication was A.R. Jalilian of the Division of Physical and Chemical Sciences.

TABLE OF CONTENTS

1. INTRODUCTION

1.1. BACKGROUND

The past decade has seen significant growth in the use of ^{68}Ga. This is attributed in part to the availability of commercial generators giving rise to a chemically useful [^{68}Ga]GaCl$_3$, thus making ^{68}Ga the first widely accessible radiometal for positron emission tomography (PET). Second, with the introduction of ^{177}Lu based radiotherapy agents, ^{68}Ga has also been used as part of a theranostic pair with ^{177}Lu to identify patients which might benefit from such ^{177}Lu therapy, and/or follow-up on treatment response. The number of clinical trials starting for ^{177}Lu and ^{68}Ga over the past two decades are noted below in Fig. 1.
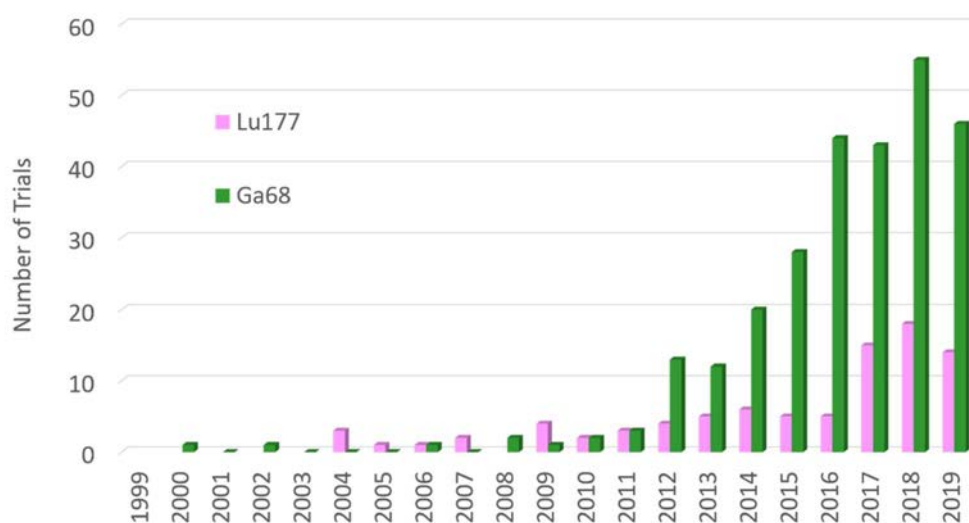
FIG. 1. Clinical trials starting by year as tabulated from clinicaltrials.gov for ^{68}Ga and ^{177}Lu (Courtesy of Ms. Gagnon, GE Healthcare, Sweden).

Despite this recently observed growth in ^{177}Lu, several reasons why one may wish to use a different therapy nuclide for the application in question include, but are not limited to wanting:

—— A longer (or shorter) lived β$^-$ emitter to best match kinetics of the tracer;
—— A higher (or lower) energy β$^-$ emitter to best match targeting environment;
—— A longer lived radionuclide to facilitate logistics;
—— A radionuclide with a matched PET nuclide;
—— A radionuclide with high specific activity;
—— A radionuclide with different decay properties (e.g. α emitter, Auger electron).

With the above characteristics in mind, the decay properties of several β$^-$ therapeutic radionuclides are listed in Table 1, of which ^{67}Cu, ^{186}Re, and ^{47}Sc have been identified as emerging nuclides of interest to the nuclear medicine community. In particular, copper and scandium have a unique property of having both β$^+$ emitting isotopes such as ^{60,61,64}Cu or ^{43,44g}Sc and β$^-$ emitting isotopes of ^{67}Cu and ^{47}Sc, thereby allowing for a true matched theranostic pairing of quantitative PET with therapy. And although there is not a suitable matching PET nuclide for ^{186}Re, rhenium and technetium are quite similar; thus, use of ^{99m}Tc based tracers pared to ^{186}Re might be well suited in regions where PET scanners are not as widely accessible. It should be cautioned that while non-matched pairs are common and have been implemented in clinical practice (e.g. ^{68}Ga/^{177}Lu), radiolabelling of the same

molecule with two different elements can, at times (but not necessarily), result in different binding affinities or biodistributions [1].

TABLE 1. EXAMPLE β⁻ NUCLIDES FOR THERNANOSTIC APPLICATIONS

Isotope	Half-life	β⁻ emission	β⁻ mean energy	Dominant γ emission	Candidate PET nuclide(s)
^{67}Cu	2.58 d	100 %	141 keV	185 keV (48.7%)	^{60}Cu, ^{61}Cu, ^{64}Cu
^{186}Re	3.72 d	92.53 %	346.7 keV	137 keV (9.4 %)	Not available
^{47}Sc	3.35 d	100 %	162.0 keV	159 keV (68.3 %)	^{43}Sc, ^{44}Sc
^{177}Lu	6.65 d	100 %	134 keV	208 keV (10.4%)	Not available
^{90}Y	2.67 d	100 %	933.6 keV	≈ 0%	^{86}Y

In reviewing similar data on 'clinicaltrials.gov' for these three nuclides (or other medically relevant isotopes of such nuclides), a similar growing trend in the past decade is observed (Fig. 2) [2]. Although the majority of such studies were diagnostic in nature, two very recent trials with ^{67}Cu, and five clinical trials with ^{186}Re are reported. However, the widespread use of ^{67}Cu, ^{186}Re and ^{47}Sc in preclinical and clinical trials continues to be a challenge due to a lack of widely established production methods. It is for this reason that a CRP was established to explore the most promising methods for producing these three radionuclides, considering both reactor and accelerator based production routes; the learnings and results of which form the basis of this publication.
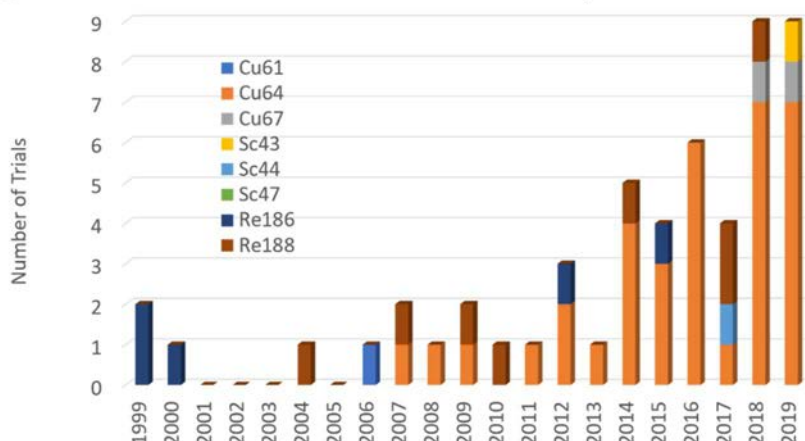
FIG. 2. Clinical trials starting by year for medically relevant Cu, Re, and Sc isotopes.

The optimal production method for a site will largely depend on the different types of available facilities (e.g. reactor/accelerator), availability of suitable particle and energy, availability of suitable target material/enrichment, as well as several other practical considerations such as yield requirements (e.g. is a site intending to produce for clinical applications, or small in vitro/pre-clinical scale). Selected candidate reactor and accelerator based production routes, many of which are discussed in further detail in this publication, are summarized in Table 2.

TABLE 2. CANDIDATE PRODUCTION ROUTES FOR ^{67}Cu, ^{186}Re, AND ^{47}Sc

Radionuclide	Installation	Candidate routes*	Nat. Ab. (%)	Q-value (MeV)
^{67}Cu	Accelerator	^{64}Ni(α,p)^{67}Cu	0.9255	-4.643
		^{70}Zn(p,α)^{67}Cu	0.61	2.618
		^{70}Zn(d,αn)^{67}Cu	0.61	0.394
		^{68}Zn(p,2p)^{67}Cu	18.45	-9.976
		^{68}Zn(γ,p)^{67}Cu	18.45	-9.976
		^{68}Zn(d,^{3}He)^{67}Cu	18.45	-4.483
		^{67}Zn(d,2p)^{67}Cu	4.04	-2.003
		^{71}Ga(p,αp)^{67}Cu	39.892	-5.244
	Reactor	^{67}Zn(n,p)^{67}Cu	4.04	0.221
^{186}Re	Accelerator	^{186}W(p,n)^{186}Re	28.43	-1.363
		^{186}W(d,2n)^{186}Re	28.43	-3.588
		^{186}W(^{3}He,t)^{186}Re	28.43	-0.600
		^{186}W(α,nt)^{186}Re	28.43	-21.177
		^{189}Os(p,α)^{186}Re	16.15	7.804
		^{192}Os(p,3nα)^{186}Re	40.78	-13.305
		^{208}Pb(p,x)^{186}Re	52.4	spallation
		^{197}Au(p,x)^{186}Re	100	spallation
	Reactor	^{185}Re(n,γ)^{186}Re	37.40	6.179
		^{187}Re(n,2n)^{186}Re	62.60	-7.360
^{47}Sc	Accelerator (Direct)	^{48}Ca(p,2n)^{47}Sc	0.187	-8.741
		^{48}Ca(d,3n)^{47}Sc	0.187	-10.966
		^{46}Ca(d,n)^{47}Sc	0.004	6.261
		^{44}Ca(α,p)^{47}Sc	2.09	-1.996
		^{50}Ti(p,α)^{47}Sc	5.18	-2.231
		^{50}Ti(d,αn)^{47}Sc	5.18	-4.455
		^{49}Ti(p,^{3}He)^{47}Sc	5.41	-11.869
		^{49}Ti(d,α)^{47}Sc	5.41	6.483
		^{48}Ti(p,2p)^{47}Sc	73.72	-11.445
		^{48}Ti(d,^{3}He)^{47}Sc	73.72	-5.951
		^{48}Ti(γ,p)^{47}Sc	73.72	-11.445
		^{47}Ti(d,2p)^{47}Sc	7.44	-2.043
		^{51}V(p,αp)^{47}Sc	99.75	-10.292
	Accelerator (Indirect)	^{48}Ca(p,d)^{47}Ca$\rightarrow^{47}$Sc	0.187	-7.727
		^{48}Ca(d,t)^{47}Ca$\rightarrow^{47}$Sc	0.187	-3.694
		^{46}Ca(d,p)^{47}Ca$\rightarrow^{47}$Sc	0.004	5.051
		^{50}Ti(p,p^{3}He)^{47}Ca$\rightarrow^{47}$Sc	5.18	-24.018
		^{50}Ti(d,αp)^{47}Ca$\rightarrow^{47}$Sc	5.18	-5.665
		^{49}Ti(p,3p)^{47}Ca$\rightarrow^{47}$Sc	5.41	-20.797
	Reactor	^{47}Ti(n,p)^{47}Sc	7.44	0.181
		^{46}Ca(n,γ)^{47}Ca$\rightarrow^{47}$Sc	0.004	11.626

*Note: routes reported herein were selected as the reaction with the lowest q value. the corresponding q value for other emission combinations can be calculated (e.g. by subtracting 2.224 MeV [d$\rightarrow$pn], 7.718 MeV [^{3}He$\rightarrow$2pn], 8.482 MeV [t$\rightarrow$p2n], 28.296 MeV [$\alpha\rightarrow$2p2n], etc)

According to IAEA database 'Cyclotrons used for Radionuclide Production'[1], over 1400 installations worldwide have abundant and accessible radioisotope production machines, and this publication covers the most practical cyclotron production methods. For reactions not addressed in this

---

[1] Database can be accessed at https://nucleus.iaea.org/sites/accelerators/Pages/Cyclotron.aspx

publication, or to seek further information (e.g. considering different energy ranges than those investigated herein), one may wish to refer to the IAEA Medical Isotope Brower[2] tool to estimate production yields and competing reactions.

Critical to radionuclide production, however, is not only the nuclear reaction; the radionuclide must additionally be isolated in a chemically useful form for subsequent radiolabelling. To this end, optimized methods for target preparation, separation chemistry, and target recycling are imperative. These technical challenges should not be underestimated and example methods/recipes and considerations to their selection are outlined in this publication.

1.2. OBJECTIVES

The objectives of this publication are to collect and summarize a collection of relevant experiences and data, including nuclear data, targetry, purification methods, and recycling (as applicable) for both accelerator and reactor based production of ^{67}Cu, ^{186}Re and ^{47}Sc as emerging β^- emitting radionuclides for therapy. The guidance provided herein represents both Member State experiences from the CRP, and prior literature, but does not intend to exclude other valuable input, should it happen to be omitted in this publication.

1.3. SCOPE

This publication aims to provide the reader hands-on information to select suitable production methods for ^{67}Cu, ^{186}Re and ^{47}Sc based on infrastructure and experience of one's facility and in consideration of yield requirements.

1.4. STRUCTURE

This publication discusses the different production routes, comparing advantages and disadvantages of reactor/accelerator routes, as well as direct/indirect production routes where applicable. Target preparation, purification techniques, and recovery of the starting material, where necessary are discussed for the different possible target materials – i.e. Zn and Ni for ^{67}Cu (Chapter 2); W for ^{186}Re (Chapter 3); and Ca, Ti, and V for ^{47}Sc (Chapter 4). Select examples of radiolabelling and aspects related to quality control (QC) are presented in the respective chapters, with additional high-level discussion of regulatory considerations presented in Chapter 5. The overall aim is to enable the reader to investigate and start their own production of these isotopes in their facilities for their respective theranostic programs.

2. ^{67}Cu PRODUCTION AND RADIOCHEMISTRY

2.1. ^{67}Cu NUCLEAR DATA

The half-life of ^{67}Cu is $T_{1/2}$=61.83 h. ^{67}Cu decays to the stable ^{67}Zn by 100% β^- decay, with a mean β^- energy of 141 keV. The decay is accompanied by emission of several intense γ lines, with the three highest intensity lines having energies of 91.3 keV, 93.3 keV and 184.6 keV with respective γ intensities of 7.00%, 16.10% and 48.7%. The decay is also followed by emission of Auger electrons.

---

[2] IAEA Medical Isotope Brower can be accessed at https://www-nds.iaea.org/relnsd/isotopia/isotopia.html

Copper-67 can be formed in several light charged particle induced nuclear reactions from Ni, Cu, Zn and Ga target materials. Reactions on Cu are not considered practical for nuclear medicine applications since the use of Cu target material would not result in high specific activity ^{67}Cu.

Charged particle reactions discussed in this publication include:

$$^{64}Ni(\alpha,p)^{67}Cu \qquad ^{70}Zn(p,\alpha)^{67}Cu \qquad ^{71}Ga(p,\alpha n)^{67}Cu$$

$$^{70}Zn(d,\alpha n)^{67}Cu$$

$$^{68}Zn(p,2p)^{67}Cu$$

$$^{68}Zn(d,^3He)^{67}Cu$$

$$^{67}Zn(d,2p)^{67}Cu$$
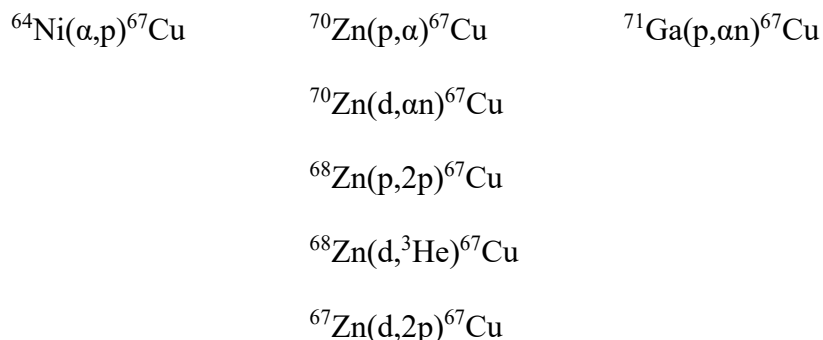
Additional noteworthy (non-charged particle based) reactions of consideration are $^{67}Zn(n,p)^{67}Cu$ and $^{68}Zn(\gamma,p)^{67}Cu$.

To compare the expected yields, and radioisotopic and cold copper impurities due to side reactions for the different production routes of ^{67}Cu, calculations were carried out on the main reactions involved in the production processes. Estimation of the expected yield of each reaction was determined by using the reaction excitation function for the nuclear reaction and the relevant stopping power of the target material. In each case, the evaluated experimental cross sections were used when they were available, otherwise the corresponding cross section data were taken from the TENDL-2017 database available online [3]. In addition to the yield of the investigated reaction routes of ^{67}Cu, the yields of the possible side reactions were also calculated to estimate the expected radioisotopic purity of ^{67}Cu and to determine the main contaminating reaction products.

Both direct and indirect (via decay) processes were considered in the calculations. The decay production includes decay chains with maximum five elements (four decay steps). The expected activity of the main reaction product, ^{67}Cu, the total number of Cu nuclei, and the total expected activity of the contaminating other copper isotopes were calculated using the end of bombardment (EOB) as a reference time. Yields were also determined after various cooling times. The cooling time was selected as an estimated time to perform the necessary chemical processing of the irradiated target material and/or to reduce the amount of the co-produced contaminating radionuclides. To enhance the production yield of ^{67}Cu, each production route requires enriched target material. In the comparison of different production routes, a 98% isotopic enrichment of the target isotope was assumed. As ^{67}Cu has the longest half-life among the radioactive copper isotopes, long irradiation times were assumed as longer irradiations reduce the relative amount of the radioisotopic contaminants. The energy window of the bombarding particles was selected to maximize the yield of the ^{67}Cu and at the same time minimize the amount of the co-produced contaminating radioisotopes. In general, production of the ^{60,61,62,66,68,69}Cu radioisotopes have negligible practical impact on the radioisotopic purity of ^{67}Cu since the half-lives of those isotopes are relatively short, and therefore, decay relatively quickly. In contrast, ^{64}Cu is the most relevant radioisotopic impurity to consider, and in most cases co-production of ^{64}Cu is unavoidable. Due to its relatively long half-life ($T_{1/2}$ =12.7 h) long cooling times (t_c=72 h) were selected for the models described below to reduce the relative amount of ^{64}Cu in the final product.

2.1.1. Ni target materials

Using stable Ni, the only feasible nuclear reaction is to produce ^{67}Cu is the ^{64}Ni(α,p)^{67}Cu reaction (Fig. 3). However, other Cu isotopes with lower mass are also co-produced on the stable Ni target isotopes.

2.1.1.1. ^{64}Ni(α,p)^{67}Cu

In the energy window of 33–9 MeV the ^{64}Ni(α,p)^{67}Cu reaction allows production of pure ^{67}Cu, since there is no co-production of ^{64}Cu on the ^{64}Ni target isotope. However, co-production of ^{64}Cu is unavoidable on the lower mass stable Ni isotopes present in the enriched ^{64}Ni target material. The enriched target material is available at high enrichment level (99.6%) and the high stopping power of α particles allows for a relatively small target thickness which in turn may simplify the target purification chemistry. In the 33–9 MeV energy window the effective target thickness is approximately 148 µm. The target processing to isolate the radiocopper is well established as it is the same as the widely used method for producing ^{64}Cu on ^{64}Ni by using proton or deuteron beams.
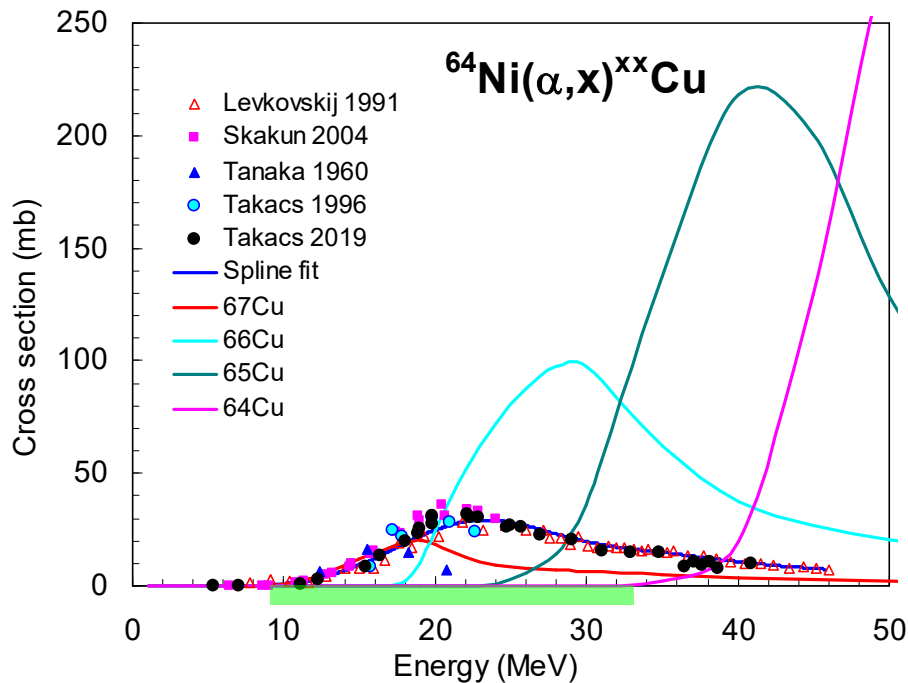
FIG. 3. Experimental and theoretical excitation function of the ^{64}Ni(α,p)^{67}Cu reaction and possible contaminating reactions (Courtesy of Mr. Takacs, Hungarian Academy of Sciences, Hungary).

A new cross section measurement of the ^{64}Ni(α,p)^{67}Cu reaction was performed in this CRP. The resulting new data confirmed the only previously available dataset above 24 MeV, as shown in Fig. 4.
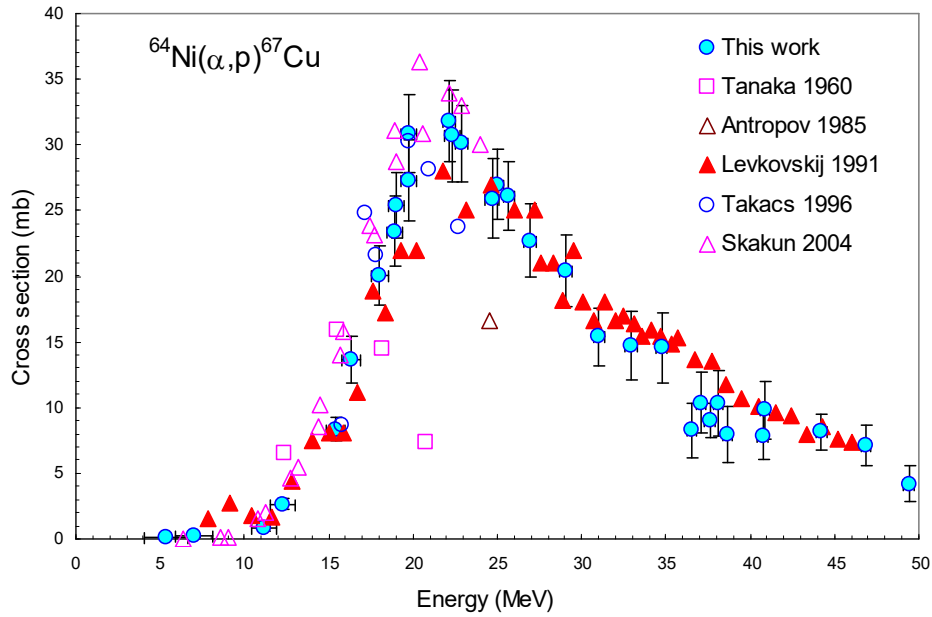
FIG. 4. A new measurement performed during the CRP confirmed the available experimental data of the $^{64}Ni(\alpha,p)^{67}Cu$ reaction (Courtesy of Mr. Takacs, Hungarian Academy of Sciences, Hungary).

Co-production of the stable ^{65}Cu isotope is also of consideration. The corresponding reaction for ^{65}Cu has a large production rate at higher energies. Therefore, from a theoretical perspective, and not considering any potential stable Cu introduced through chemical processing, the expected specific activity of ^{67}Cu decreases by increasing bombarding energy. In the 33–9 MeV energy window, approximately 19 MBq/µA of ^{67}Cu can be produced during a 24 h long irradiation of 98% enriched ^{64}Ni target. In consideration of theoretical specific activity, the estimated relative number of other copper isotopes (i.e. atomic ratio of ^{67}Cu to other Cu isotopes) present after 72 h cooling time reaches 73% due to mainly the co-produced stable $^{63,65}Cu$ isotopes.

The disadvantage of this reaction is the limited availability of α beams and the relatively low reaction yield. In the energy range of 36–9 MeV a 0.53±0.096 MBq/µAh thick target yield was experimentally measured which matches well with the 24 h calculations described above.

2.1.2. Cu target materials

Although ^{67}Cu can technically be produced via the $^{65}Cu(\alpha,2p)^{67}Cu$ reaction, this production route is not considered to be applicable for nuclear medicine applications since it would result in an unsuitably low specific activity ^{67}Cu.

2.1.3. Zn target materials

The reactions $^{70}Zn(p,\alpha)^{67}Cu$, $^{70}Zn(d,\alpha n)^{67}Cu$, $^{68}Zn(p,2p)^{67}Cu$, $^{68}Zn(d,^{3}He)^{67}Cu$ and $^{67}Zn(d,2p)^{67}Cu$ were considered for production of ^{67}Cu.

2.1.3.1. $^{70}Zn(p,\alpha)^{67}Cu$

The $^{70}Zn(p,\alpha)^{67}Cu$ reaction has a low practical threshold energy of ~7 MeV. In the energy range of 24–8 MeV there is no co-production of long lived copper contaminant isotopes in ^{70}Zn. However, production of stable ^{65}Cu isotope starts above 14 MeV, which may influence the specific activity of ^{67}Cu from a theoretical perspective (i.e. not considering any potential stable Cu or other competing

7

metals introduced through chemical processing). Use of highly enriched ^{70}Zn for the target material is recommended. Possible Cu impurities may also come from reactions on the other stable Zn isotopes present in minor amounts in the target material. The currently available commercial maximum isotopic enrichment of ^{70}Zn is 95.47%. This highly enriched ^{70}Zn is expensive, making the recovery and re-use of the irradiated target material an important task. Using this target material, ~113 MBq/µA activity of ^{67}Cu can be obtained at EOB after a 24 h irradiation time. To reduce the activity of the co-produced ^{64}Cu below 1% requires approximately 3 days of cooling, which also reduces the activity of the ^{67}Cu to approximately 50 MBq/µA. In the 24–8 MeV energy window, the expected relative amount of the co-production of ^{63,65}Cu isotopes is approximately 60% of total Cu after 72 h cooling time. A longer irradiation time would increase the expected activity of ^{67}Cu but decrease the specific activity due to the co-produced stable ^{63,65}Cu isotopes. Fig. 5 presents an experimental and theoretical excitation function of the ^{70}Zn(p,α)^{67}Cu reaction with possible contaminating reactions.
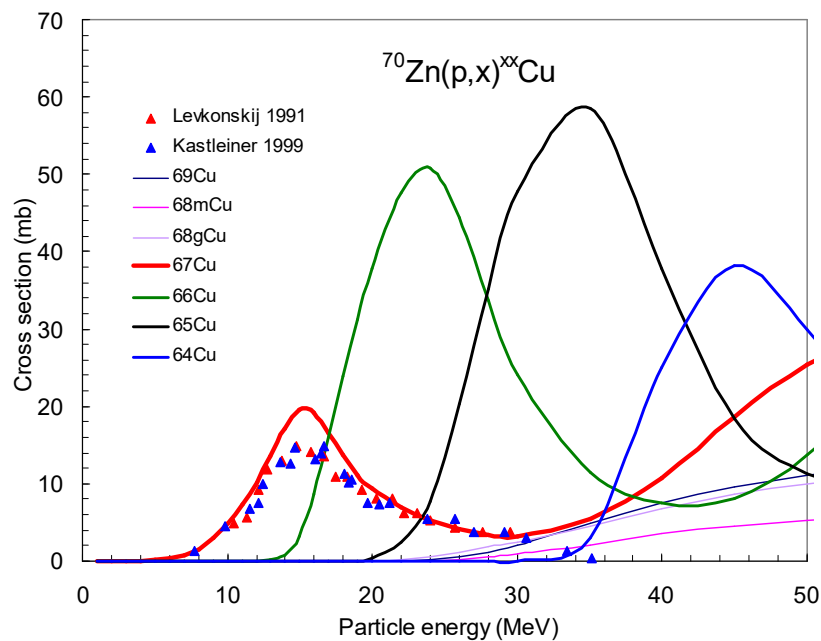
FIG. 5. ^{70}Zn(p,α)^{67}Cu reaction (Courtesy of Mr. Takacs, Hungarian Academy of Sciences, Hungary).

For the 24–8MeV proton energy window, a 1.15 mm effective target thickness is required. Co-production of the long lived ^{65}Zn is possible in this energy window due to reactions of the ^{66,67,68}Zn isotopes present in the target in minor amounts. Accumulation of ^{65}Zn is expected in the enriched ^{70}Zn target material during cycles of recovery and reuse.

2.1.3.2. ^{70}Zn(d,αn)^{67}Cu

The practical energy for producing ^{67}Cu via the ^{70}Zn(d,αn)^{67}Cu reaction begins at ~7 MeV. In the energy range of 25–7 MeV there is no co-production of contaminant Cu isotopes on ^{70}Zn. The threshold energy for production of ^{64}Cu from ^{70}Zn is nearly 30 MeV, thus any ^{64}Cu impurity likely comes from reactions of the other stable Zn isotopes present in minor amounts in the target material. For this reason, a highly enriched target is recommended. In comparison with proton beams, the required effective target thickness is lower; 776 µm instead of 1.15 mm. There is only one experimental data set for the cross sections of this deuteron reaction measured up to 20 MeV. The maximum of the excitation function is also around 20 MeV, which indicates that additional experimental data are required at higher energies. In the 25–7 MeV energy window, the expected yield of ^{67}Cu after 24 h irradiation at EOB is approximately 123 MBq/µA, while the activity of ^{64}Cu

is approximately 15 MBq/µA. By letting the irradiated target cool for 3 days, the activity ratio of ^{64}Cu contamination decreases below 1%, while the activity of ^{67}Cu would also decay to approximately 55 MBq/µA which is in the same range as yields from proton bombardment. However, the amount of co-produced stable ^{63,65}Cu is less; therefore, the specific activity of ^{67}Cu produced by deuteron bombardment on ^{70}Zn is potentially higher than that for proton bombardment. By increasing the bombarding energy to 30 MeV, the expected activity of ^{67}Cu would increase by approximately 30% but at the same time, the increased co-produced of stable copper would increase significantly. Fig. 6 presents an experimental and theoretical excitation function of the ^{70}Zn(d,αn)^{67}Cu reaction with possible contaminating reactions.
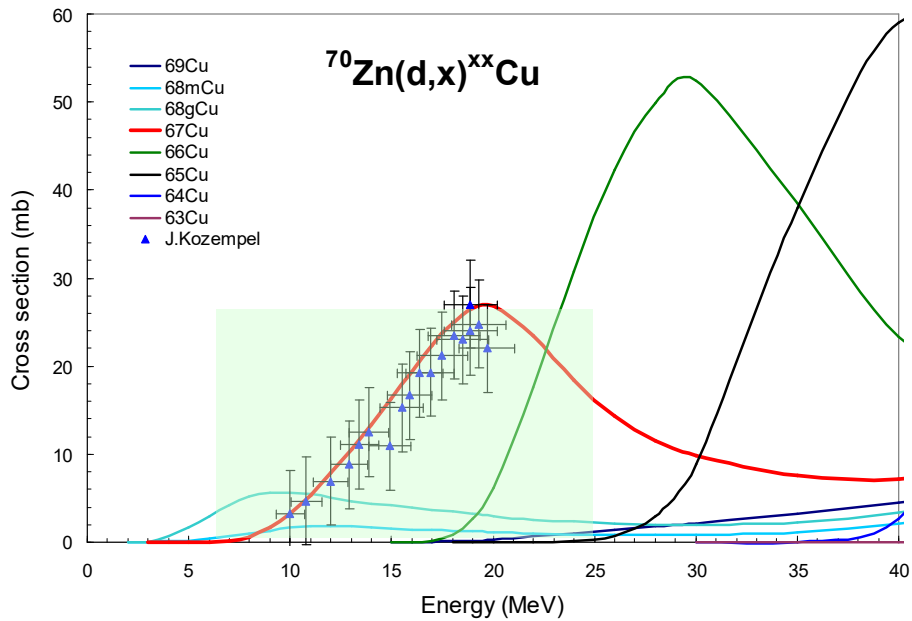

FIG. 6. ^{70}Zn(d,αn)^{67}Cu reaction (Courtesy of Mr. Takacs, Hungarian Academy of Sciences, Hungary).

2.1.3.3. ^{68}Zn(p,2p)^{67}Cu

This production route on ^{68}Zn requires higher proton energies compared with the reactions above. The ^{68}Zn(p,2p)^{67}Cu reaction has a threshold energy of E_{th}=10.1 MeV, but this reaction is practically feasible from about 20 MeV and can be used up to proton energies of ~200 MeV. Evaluated experimental cross section data are available up to 100 MeV [4]. New experimental data were measured in the frame of this CRP up to 70 MeV [5]. Co-production of ^{64}Cu as a contaminant isotope is present in the entire energy range with varying intensities. The ^{64}Cu contamination level can be reduced by considering specific proton energy windows but cannot be avoided. In order to reach a higher radioisotopic purity of ^{67}Cu, a long cooling time (e.g. several days) is mandatory. The main advantage of this production route is that the required ^{68}Zn target material which is available at high enrichment levels (>99%) and is much less expensive than ^{70}Zn. As a consequence of higher energy protons required than reactions above, significantly more target material is needed, unless a narrow energy window is selected. The range of a 100 MeV proton beam in a Zn target is approximately 17 mm. For a proton energy window of 50 to 38 MeV, the effective target thickness is 1.89 mm. Using this energy window, approximately 166 MBq/µA ^{67}Cu can be produced during a 24 h irradiation time. The activity of the co-produced ^{64}Cu at EOB is estimated to be around 700 MBq/µA, which can be reduced to approximately 7% after 4 days of cooling time. Four days of cooling time reduces the activity of ^{67}Cu to approximately 57 MBq/µA. Co-production of stable ^{63,65}Cu are unavoidable and the production of these stable isotopes is considerably high. In fact, the expected amount of ^{63,65}Cu

nuclei after the 4 day cooling time is more than 20 times higher than [67]Cu nuclei. The high energy proton bombardment also increases the production yield of [65]Zn in the target; therefore, the activity of [65]Zn would quickly build up in the recovered target material after several irradiations. Fig. 7 presents an experimental and theoretical excitation function of the [68]Zn(p,2p)[67]Cu reaction and potential contaminating reactions.
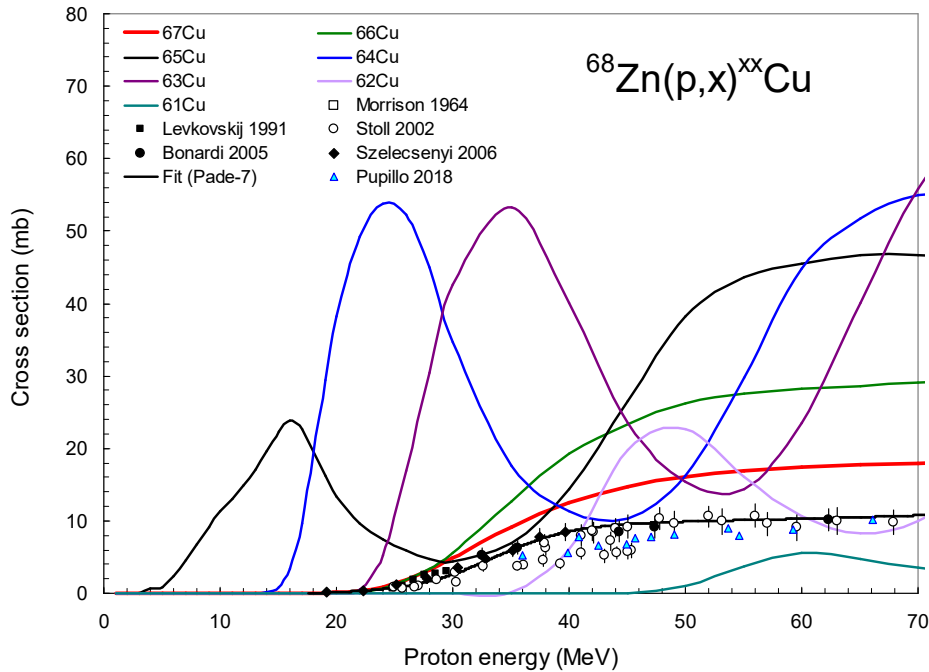
FIG. 7. *[68]Zn(p,2p)[67]Cu reaction (Courtesy of Mr. Takacs, Hungarian Academy of Sciences, Hungary).*

2.1.3.4. [68]Zn(d,[3]He)[67]Cu

For this production route, no reasonable experimental data are currently available. The theoretical prediction shows that ^{64}Cu is produced via several reaction channels, with peaks at ~30 MeV and 70 MeV, and has and a local minimum at ~50 MeV. Co-production of ^{64}Cu cannot be avoided but using an energy window of approximately 49 MeV the yield of the co-produced ^{64}Cu can be minimized. Using a deuteron energy window from 57 to 45 MeV, a [67]Cu yield of 317 MBq/µA can be predicted at EOB, with ^{64}Cu yield of 337 MBq/µA following a 24 h irradiation period.

After 72 h of cooling time, the relative activity of ^{64}Cu is reduced below 5%, but the activity of [67]Cu also decreases to 141 MBq/µA. The required effective target thickness for this energy window is approximately 486 µm, which is about four times less than what is necessary for 50–38 MeV energy proton bombardment of [68]Zn. The advantage of the deuteron bombardment compared with the proton irradiation are: reduced mass of target material, higher EOB activity of [67]Cu, lower ^{64}Cu contamination level, and potential for higher specific activity due to lower amount of co-produced [63,65]Cu isotopes. The disadvantage of this production route is the required high energy deuteron beam, which is not a common option for most cyclotrons used for medical radionuclide production. Another consequence of the high energy deuteron irradiation of the [68]Zn target material is the co-production of [65]Zn which is unavoidable, leading to a buildup of [65]Zn activity in the recycled target material. Figure 8 shows an experimental and theoretical excitation function of the [68]Zn(d,[3]He)[67]Cu reaction and possible contaminating reactions.
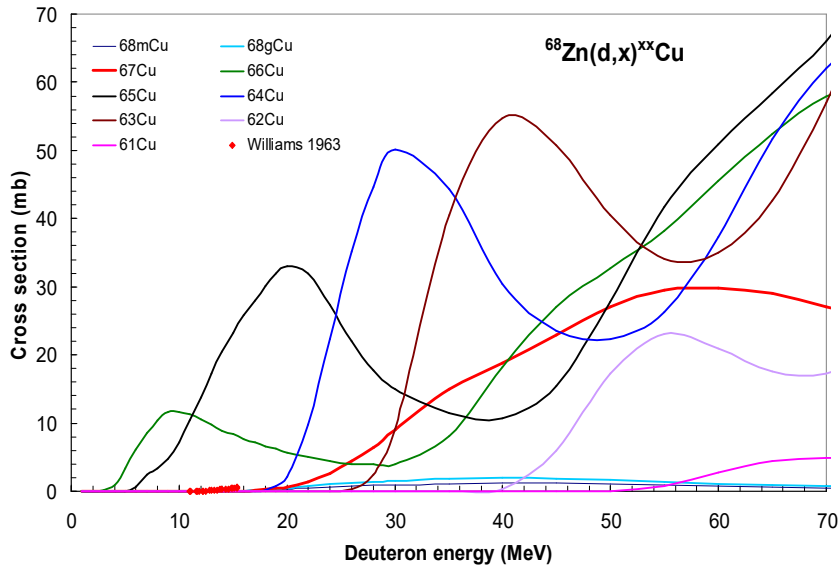
FIG. 8. $^{68}Zn(d,^3He)^{67}Cu$ reaction (Courtesy of Mr. Takacs, Hungarian Academy of Sciences, Hungary).

2.1.3.5. $^{67}Zn(d,2p)^{67}Cu$

The predicted cross sections for the $^{67}Zn(d,2p)^{67}Cu$ reaction are lower than the ^{64}Cu production cross sections over the entire useful energy range; therefore, the expected ^{67}Cu yield is lower than the yield of ^{64}Cu in any selected energy window. Due to the high ^{64}Cu contamination level, this reaction is not practical for the production of ^{67}Cu. A comparison with the other production routes is shown in the Table 3 below for the 44–30 MeV energy window. Figure 9 shows an excitation function of the $^{67}Zn(d,2p)^{67}Cu$ reaction and possible contaminating reactions.
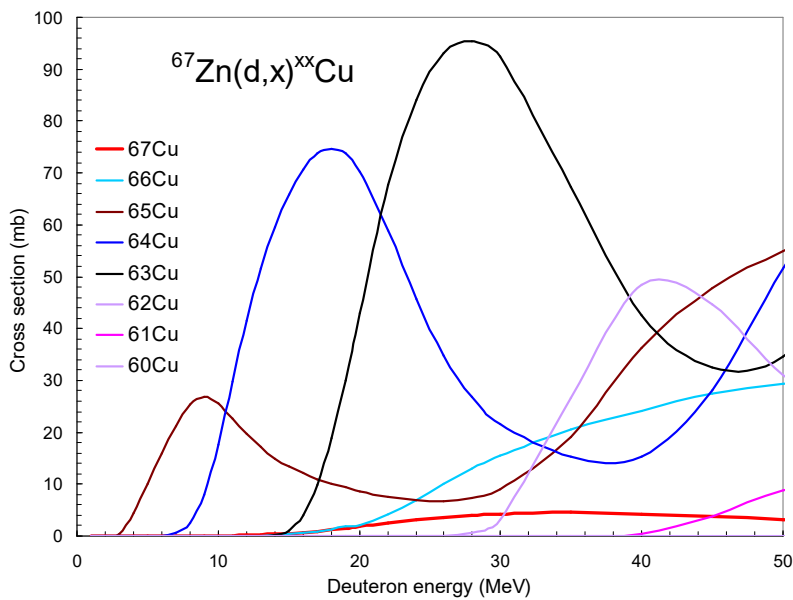
FIG. 9. $^{67}Zn(d,2p)^{67}Cu$ reaction (Courtesy of Mr. Takacs, Hungarian Academy of Sciences, Hungary).

2.1.3.6. $^{71}Ga(p,\alpha n)^{67}Cu$

Production of ^{67}Cu using a gallium target requires isotopically enriched ^{71}Ga as a target material. Although, in principle, both of the stable Ga isotopes are suitable for production of ^{67}Cu in proton or

deuteron bombardment, reactions on ^{69}Ga should be excluded due to the expected low cross section of the ^{69}Ga (p,3p) ^{67}Cu reaction and high yield of the co-produced ^{64}Cu radionuclide.

The practical energies for producing usable quantities of ^{67}Cu via the ^{71}Ga(p,αn)^{67}Cu reaction begin at around 20 MeV, while the threshold energy of the ^{71}Ga(p,αnt)^{64}Cu reaction is ~23 MeV, with meaningful production starting at ~40 MeV. Therefore, the 40–20 MeV energy window will optimize ^{67}Cu while minimizing ^{64}Cu. In this 40–20 MeV proton energy window approximately 12 MBq/µA ^{67}Cu can be expected after a 24 h irradiation period on a 98% enriched ^{71}Ga target. The disadvantages of this reaction are: the small cross sections, resulting low yield of the reaction, the relatively high ^{64}Cu contamination level (3.6% after 72 h cooling time), and the low melting point of gallium (29.8°C) which makes the target preparation difficult. Using a gallium alloy with a higher melting point would likely increase the tolerable beam current but would decrease the reaction yield. Additionally, co-production of stable ^{65}Cu is unavoidable, which may decrease the specific activity of ^{67}Cu. Figure 10 shows an experimental and theoretical excitation function of the ^{71}Ga(p,αn)^{67}Cu reaction and possible contaminating reactions.
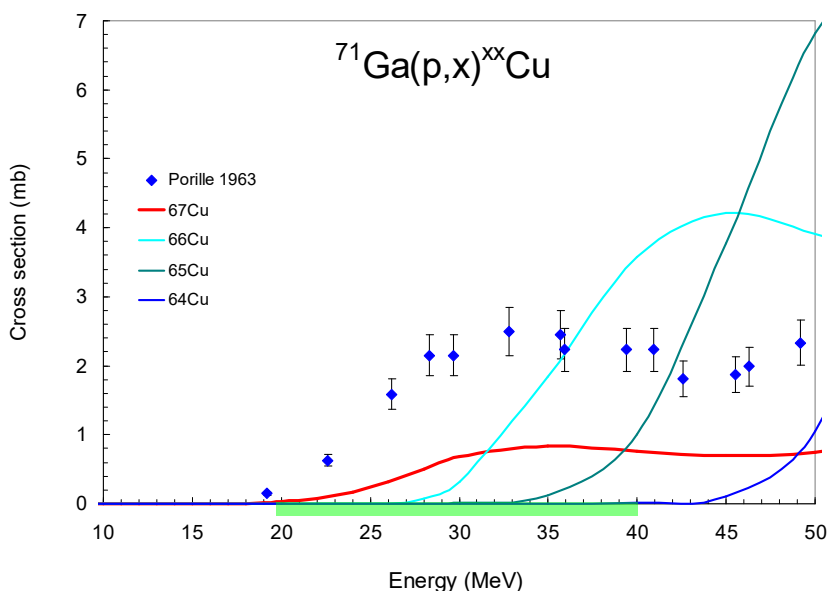
FIG. 10. ^{71}Ga(p,αn)^{67}Cu reaction (Courtesy of Mr. Takacs, Hungarian Academy of Sciences, Hungary).

2.1.4. Comparison of cyclotron production routes of ^{67}Cu

Comparison of cyclotron production routes of ^{67}Cu on Ni, Zn and Ga enriched targets was modelled at the following fixed irradiation parameters:

— Irradiation time: 24 h and 72 h;
— Beam current: 1 µA;
— Cooling time: 72 h;
— Target enrichment: 98%.

The predicted values for the expected production yield of ^{67}Cu and the radiocopper (^{64}Cu) contamination level as well as the amount of co-produced stable ^{63,65}Cu isotopes are listed in Tables 3 and 4 for 24 h and 72 h irradiation times.

TABLE 3. COMPARISON OF CYCLOTRON PRODUCTION ROUTES OF ^{67}Cu ON Ni, Zn AND Ga TARGETS *(24 h irradiation time, 1 eµA beam current, 72 h cooling time)*

	E_{in} (MeV)	E_{out} (MeV)	Target isotope (98%)	Effective target thickness (µm)	^{67}Cu activity at EOB (MBq)	^{67}Cu activity after cooling (MBq)	Relative activity of other Cu isotopes to ^{67}Cu after cooling (%)	Relative number of atoms of other Cu to ^{67}Cu after cooling (%)
^{64}Ni(α,p)^{67}Cu	33	9	^{64}Ni	148	18.9	8.4	1.8	73
^{70}Zn(p,α)^{67}Cu	24	8	^{70}Zn (95%)	1 149	113	50.6	1.3	60
^{68}Zn(p,2p)^{67}Cu	50	38	^{68}Zn	1 892	166	74	18.7	1 560
^{70}Zn(d,αn)^{67}Cu	25	7	^{70}Zn (95%)	776	123	54.9	0.55	26
^{68}Zn(d,^{3}He)^{67}Cu	57	45	^{68}Zn	486	317	141	4.7	690
^{67}Zn(d,2p)^{67}Cu	44	30	^{67}Zn	1 127	47	21	55	5 137
^{71}Ga(p,αp)^{67}Cu	40	20	^{71}Ga	2905	12.5	5.6	3.6	66

TABLE 4. COMPARISON OF CYCLOTRON PRODUCTION ROUTES OF ^{67}Cu ON Ni, Zn AND Ga TARGETS *(72 h irradiation time, 1 eµA beam current, 72 h cooling time)*

	E_{in} (MeV)	E_{out} (MeV)	Target isotope (98%)	Target thickness (µm)	^{67}Cu activity at EOB (MBq)	^{67}Cu activity after cooling (MBq)	Relative activity of other Cu isotopes to ^{67}Cu after cooling (%)	Relative number of atoms of other Cu to ^{67}Cu after cooling (%)
^{64}Ni(α,p)^{67}Cu	33	9	^{64}Ni	148	44.4	19.8	1.0	100
^{70}Zn(p,α)^{67}Cu	25	5	^{70}Zn (95%)	1149	266	119	0.72	77
^{68}Zn(p,2p)^{67}Cu	50	38	^{68}Zn	1892	391	174	10.7	2015
^{70}Zn(d,αn)^{67}Cu	25	7	^{70}Zn (95%)	776	289	129	0.32	33
^{68}Zn(d,^{3}He)^{67}Cu	57	45	^{68}Zn	486	744	332	2.7	882
^{67}Zn(d,2p)^{67}Cu	44	30	^{67}Zn	1127	110	49	32	6556
^{71}Ga(p,αp)^{67}Cu	40	20	^{71}Ga	2905	29	13	2.1	84

For the 24 h irradiation time, the ^{70}Zn(d,αn)^{67}Cu and ^{70}Zn(p,α)^{67}Cu reactions proved to be the cleanest production routes for ^{67}Cu. The (d,αn) and (p,α) reactions also have low threshold energies, therefore a relatively low energy window can be selected for irradiation. The two reactions provide similar ^{67}Cu yield and require similar energy window, but the deuteron option for cyclotrons are not always available. Enriched ^{64}Ni is not as expensive as the ^{70}Zn, the ^{64}Ni(α,p)^{67}Cu reaction requires less target material and this production route provides relatively pure but lower ^{67}Cu activity.

For higher energy machines the ^{68}Zn(p,2p)^{67}Cu and ^{68}Zn(d,^{3}He)^{67}Cu reactions can be used to produce ^{67}Cu. These production routes provide higher production yield of ^{67}Cu but at the same time, the level of co-produced contaminating Cu nuclides is also higher.

2.2. ^{67}Cu PURIFICATION

2.2.1. Separation and purification of ^{67}Cu from enriched zinc target material

Copper-67 can be produced by the nuclear reaction ^{68}Zn(p,2p)^{67}Cu as described above using high energy protons (>45 MeV). ^{67}Ga is also co-produced when using this method. A typical target may consist of several grams of enriched ^{68}Zn electroplated on silver or gold layer pre-electroplated on copper support. Ion exchange resin (Dowex 50 × 4 200 mesh) can be used to separate enriched ^{68}Zn and ^{67}Cu from co-produced ^{67}Ga using 9N HCl. Next, as an example, ^{68}Zn is separated from ^{67}Cu in a second step using ion exchange resin (Dowex 1 × 8) preconditioned with 6N HCl. After loading the mixture onto the resin, ^{67}Cu is eluted from the column using 2N HCl, then ^{68}Zn is eluted from the column by 0.05N HCl.

However, separation of a large amount of ^{68}Zn using ion exchange resin or similar agents can yield poor results due to overloading of ionic species beyond the capacities of those separation materials. Thus, co-precipitation methods have been investigated using H_2S and Ag^+ as alternative methods to isolate ^{67}Cu from large amounts of ^{68}Zn and other metallic impurities. H_2S/Ag^+ co-precipitation agents yield CuS which can be re-dissolved in acidic media. As an example, this process was repeated twice, completed within 3 h, and ^{67}Cu purified by the above method showed a recovery efficiency and chemical purity comparable to conventional column separation techniques. As ^{67}Cu has a considerably long half-life of 2.58 days and targets often require a cooling time to allow for the decay of ^{64}Cu to increase the radioisotopic purity, fast chemical processing is not essential for ^{67}Cu. However, short processing times can enable a robust process, particularly in routine operations, and may contribute to overall success in daily production.

Zinc-70 can be used for ^{67}Cu production via the nuclear reaction ^{70}Zn(p,α). As an example, a 2.3g electroplated ^{70}Zn target was dissolved in 9 mL of concentrated HCl and the resulting solution was evaporated at 90°C for 40 min. Next, the ^{70}Zn target residue was re-dissolved in 380 mL of ultra-high purity water and 2 mL of hydrazine hydrate, to which 19 mL of 10N NaOH was then added to the target solution prior to purification. Copper-67 and ^{65}Zn were eluted using 10 mL of 9M HCl (from 2×5 mL fractions), while ^{66}Ga remained on the column. Eluted fractions were combined and then re-loaded on to an anion exchange column (AG1X8, 100-200 mesh, 3g). Copper-67 was eluted using 3 to 4 mL of 2M HCl, whereas ^{65}Zn remained on the column. Radionuclidic purity of ^{67}Cu was 99.9% as assessed with an HPGe detector.

^{67}Zn(n,p)^{67}Cu nuclear reaction can also be used for ^{67}Cu production using fast neutrons. This production mode of ^{67}Cu used enriched [^{67}Zn]ZnO in a nuclear reactor. Separation of the produced Cu from target materials and impurities was accomplished using ion exchange chromatography with Bio-Rad® AG1X8 resin which showed 94% chemical separation yield with a ^{67}Cu radionuclidic purity of more than 99.8%.

Another proposed processing of irradiated enriched zinc target for the separation of produced ^{67}Cu is a solvent extraction technique. The solution of the irradiated target in 0.5M HCl (25 mL) was extracted in 0.01% dithizone in CCl_4. The organic layer was carefully separated from the aqueous layer and subsequently, ^{67}Cu activity was back extracted from organic medium to a mixture of 23 mL of 7.2M HCl and 2 mL of 30% (v/v) H_2O_2. After the back extraction process, the aqueous solution was evaporated to near dryness and re-constituted in de-ionized water. The process was repeated twice and ^{67}Cu was obtained as [^{67}Cu]CuCl$_2$ solution in dilute HCl medium. The separation efficiency was 92.0%. Radiochemical purity of ^{67}Cu in the form of Cu^{2+} ions was 97.3% as determined by paper chromatography technique.

14

2.2.2.   Separation and purification of ^{67}Cu from enriched nickel

Separation chemistry for ^{67}Cu produced by irradiation of a ^{64}Ni target can be performed using the same set-up built for a typical proton induced ^{64}Cu production/separation, which also uses the same target material. Since ^{64}Cu production has been widely implemented, ^{67}Cu production with the ^{64}Ni target would be an option for the institutes with access to both α and proton beams that have established the protocols for the production of ^{64}Cu.

Recommended ^{67}Cu separation chemistry, similar to that reported for ^{64}Cu, is based on ion exchange techniques, in which two options are feasible; i.e. using (a) cation exchange resin with organic solvent based eluates, or (b) anion exchange resin alone, or coupled with chelating resin. Ionic copper typically shows +2 valency (Cu^{2+}) and has a high affinity to many types of cation exchange resin. However, other metallic ions, including target material and by-products, also show similar affinity to cation exchange resins, and thus, optimized conditions for chromatographic separation are required. Organic solvents mixed with acids, e.g. acetone/HCl, at various ratios are often used as the eluates with varying distribution coefficients for each transition metal. Thus, each ion can be isolated from others by changing the composition of the eluate. The mechanism, as well as data for distribution coefficients, can be found elsewhere [6, 7]; briefly, the hydration field around the cation is weak enough to allow the replacement of water in the coordination sphere by anions such as Cl^- and NO_3^-, and organic solvents can alter this replacement. Thus, the affinity of each ion to cation exchange resin can be changed by altering the solvent mixing ratio and the concentration of acid.

Alternatively, when using HCl, HNO_3, or other acids, anionic species, like Cl^- or NO_3^-, can coordinate with Cu^{2+} and form an anionic complex. The Cu complex with rich anions would show high affinity to anion exchange resin. By employing the above ionic chemistry, we can isolate ^{67}Cu from a bulky amount of ^{64}Ni with appropriate eluents.

All reagents used in the process should be the highest chemical purity available, because labelling processes with ^{67}Cu are easily affected by not only the specific activity of ^{67}Cu, but also the presence of other metallic impurities. The reagents include any acids, pure water for dilution, reagents for column preparation, and target material itself. Chemicals of semiconductor grade, ultra-trace analysis grade, or reagents at the highest purity in series products should be selected. Possible contaminants which impact the process are in trace levels (ppb or ppt), and thus this level of purity may be difficult to obtain. Consequently, an in-house generation system of ultrapure water may show insufficient quality in some cases.

Nickel-64 as usually purchased/available contains significant amounts of many metallic elements including cold Cu and Fe. Therefore, pre-cold run(s) including separation with 'fresh' ^{64}Ni should be carried out to reduce impurities, and the recovered ^{64}Ni in the recovered fraction to prepare the target to be irradiated. In this protocol, an optimized recycling system for ^{64}Ni should be established, and typically, the repeated use of recycling target contributes to better quality of ^{67}Cu in subsequent runs. In addition, appropriate washing of materials for the setup (e.g. glassware) as a post-production procedure is mandatory to keep the system clean, and to maintain the quality of ^{64}Ni and ^{67}Cu at high level.

As mentioned above, there are two possible pathways to separate ^{67}Cu, either anion or cation exchange resin, whereby the main difference between them can be found in the elution profile; namely the ^{67}Cu fraction elutes prior to ^{64}Ni by the cation resin method [8, 9], or in contrast, ^{64}Ni elutes before ^{67}Cu when using the anion resin method [10, 11]. Since both pathways have attractive and negative points from a practical point of view, the selection of established protocols will depend on the existing

setup, accessibility of commercial setups, regulations, waste managements, and/or associated cost in each institute or country. A comparison is shown in Table 5.

TABLE 5. COMPARISON BETWEEN CATION AND ANION EXCHANGE RESIN FOR ^{67}Cu PURIFICATION

	Cation	Anion
Resin	AG50W-X8 or equivalent	AG1-X8 or equivalent; or AG1-X4 + Chelex-100
Elution profile	Zn → Cu → Ni → Co	Ni → Co → Cu
Eluate for ^{67}Cu	2M HCl: acetone (1:9), 30 mL	Water or 0.5M HCl, 10 mL or 0.5M HCl, 20 mL
Preparation	Evaporation needed reconstitutable in any media	Ready to use in aqueous form

As most of radiocopper applications employ chelation chemistry, many elements including Ni^{2+} may compete with ^{67}Cu for a specific chelator and consequently decrease the labelling efficiency. It is widely known as an experimental experience in preparative chromatography that every peak shows a tail after the fraction appeared, even if the appropriate eluate is applied; such tailing is in proportion to the loaded amounts of both solute and volume. In typical radionuclide productions, the dominant species existing in separation system comes from the target material, which may reach up to several hundred milligrams in weight for instance. Therefore, the fraction of Ni^{2+} has the largest risk of tailing on the preparative chromatography, and large amount of eluate, as well as processing time, would be needed to collect the precious material of ^{64}Ni as much as possible, and/or to reduce the Ni^{2+} contamination in the following fraction(s). Nevertheless, because an expected yield of ^{67}Cu is relatively low by this activation channel, higher specific activity of ^{67}Cu with minimal contaminants is important for efficient radiolabelling.

An example protocol to separate $^{67/64}$Cu by using cation exchange resin:

(a) Dissolve target material with 6M HNO$_3$ (2 mL) at 120°C;
(b) Dilute crude ^{67}Cu/^{64}Ni mixture with 5 volume of ultra-pure water (10 mL) → 1M HNO$_3$;
(c) Apply crude ^{67}Cu onto AG50W-X8 (15 mL wet resin column);
(d) Wash the column with 100 mL of 0.5M HCl: acetone (2:8) to remove ^{65}Zn;
(e) Collect fraction of ^{67}Cu with 75 mL of 2M HCl: acetone (1:9);
(f) Evaporate ^{67}Cu fraction to dryness;
(g) Reconstitute ^{67}Cu residue in 10 mL of ultra-pure water to obtain as the final product;
(h) Wash the column with 80 mL of 5M HCl: acetone (1:9) to remove ^{55,61}Co;
(i) Wash the column with 50 mL of ultra-pure water to remove acetone from the system;
(j) Collect fraction of ^{64}Ni with 60 mL of 2M HCl;
(k) Wash the column with 10 mL of ultra-pure water to remove any acidic leftover.

The final ^{67}Cu product can be obtained within 1 to 2 h through the above processes of (a) to (g). Subsequent procedures of (h) to (k), which can be run any time after production, are mandatory to collect ^{64}Ni with negligible amounts of contaminants, as well as to clean up the system for making work friendly condition.

Example protocols to separate $^{67/64}$Cu by using anion exchange resin:

(a) Dissolve target material with 6M HCl (10 mL) at 90°C;

16

(b) Evaporate crude ^{67}Cu/^{64}Ni mixture to dryness;
(c) Reconstitute ^{67}Cu residue in 3 mL of 6M HCl;
(d) Apply crude ^{67}Cu solution onto AG1-X8 (3 mL wet resin volume);
(e) Collect ^{64}Ni fraction with 15 mL of 6M HCl;
(f) Collect fraction of ^{67}Cu with 8 to 10 mL of pure water or 0.5M HCl.

Alternatively:

(a) Dissolve target material in 40 mL of 8M HCl + 5 mL of conc. HNO$_3$ at 50°C;
(b) Apply crude ^{67}Cu onto AG1-X4 (14 mL wet resin volume);
(c) Collect ^{64}Ni fraction with 6→2M HCl/250 min gradient (approx. 10 to 50 mL);
(d) Collect Co + ^{67}Cu fraction with the same eluant and gradient (approx. 70 to 150 mL);
(e) Apply Co + ^{67}Cu fraction onto Chelex-100 (21 mL wet resin volume);
(f) Wash the column with 20 mL of 0.1M HCl to remove Co^{2+};
(g) Collect ^{67}Cu fraction with 20 mL of 0.5M HCl.

2.3. ^{67}Cu QUALITY CONTROL

2.3.1. Radionuclidic purity

The radionuclidic purity of ^{67}Cu solution is determined by γ spectrometry using an HPGe detector coupled with a multichannel analyser.

2.3.2. Radiochemical purity

Radiochemical purity of ^{67}Cu in the form of Cu^{2+} ions can be determined by paper chromatography technique.

2.3.3. Chemical purity

In routine ^{67}Cu production anodic stripping voltammetry can be used for trace metals analysis [12]. ICP–atomic emission spectroscopy analysis can be used to determine the trace metals concentration in the produced ^{67}Cu bulk. Caution is warranted if using ICP–mass spectrometry, in particular if analysing material which is not of natural isotopic abundance (e.g. the target material). Less sensitive, but nevertheless allowing sub ppm analysis, and may be useful for development purposes, are the commercially available colorimetric test kits (e.g. for Zn, Fe, Ni, etc.).

3. ^{186}Re PRODUCTION AND RADIOCHEMISTRY

3.1. ^{186}Re NUCLEAR DATA

Rhenium-186 decays to stable ^{186}Os with a half-life of 3.78 d by emission of β$^-$ particles having maximum energies 939 keV (22%) and 1 077 keV (77%). It also emits γ ray of 137.2 keV (9.5%), making it an attractive radionuclide for cancer theranostics. Both ^{186g}Re (T$_{1/2}$; 3.78 d) and ^{186m}Re (T$_{1/2}$; 2.0×10^5 y) exist. As the metastable state is of little relevance this publication uses ^{186}Re to denote the ground state. ^{186}Re can be produced following a variety of processes using both nuclear reactor and cyclotron or particle accelerator, as summarized in Table 6.

In a nuclear reactor, ^{186}Re can be produced by ^{185}Re(n,γ)^{186}Re [13], and ^{187}Re(n,2n)^{186}Re [14] routes. However, these reactions lead to the production of ^{186}Re in a carrier-added form with low specific activity. For the development of receptor-specific radiopharmaceuticals for targeted tumour therapy, radionuclides having high specific activity are desirable. ^{186}Re can be conveniently produced in a no carrier added (NCA) form by charged particle (p, d, or ^{3}H) and ^{186}W target [15]. Among the various possible routes, ^{186}W(d,2n)^{186}Re has been found to be most convenient [16]. Apart from these, production of NCA ^{186}Re has also been reported following other routes such as ^{186}W(^{3}He,x)^{186}Re and ^{186}W(α,x)^{186}Re [17], spallation of ^{208}Pb [18] or ^{197}Au [19] using ^{1}H as a high energy projectile. A review of the literature revealed that several works were carried out for the production of ^{186}Re via light charged particles irradiations on a tungsten target [16, 20–24]. In such studies, excitation functions for the residual radionuclides of ^{nat}W(p/d,x) nuclear processes were measured, physical yields were deduced towards the production of NCA ^{186}Re. However, close scrutiny of these studies reveals that a considerable degree of discrepancy in results, even within the same excitation energy. However, it is possible to correct the reported data or reduce the discrepancy by using the updated value of some relevant parameters such as γ ray intensity, monitor reaction cross-sections, target abundance etc. that are generally available in the original publications. On the other hand, corrections on time parameters such as half-lives are difficult due to lack of information related to the irradiation, cooling, and measurement time [16].

TABLE 6. STATUS OF THE LITERATURE DATA FOR THE PRODUCTION OF ^{186}Re

Production route	Process	Target	Abundance (%)	Cross section	Reference
Reactor	Neutron capture (n,γ)	^{185}Re	37.4	112 b	Several studies
	Neutron activation (n, 2n)	^{187}Re	62.6	2 b	[14]
Cyclotron	Proton activation (p, n)	^{186}W	28.43	~100 mb at 12 MeV	Several studies
	Deuteron activation, (d, 2n)	^{186}W	28.43	~600 mb at 15 MeV	Several studies
	Helium-3 activation, (^{3}He,x)	^{186}W	28.43	~240 mb at 32 MeV	[17]
	Helium-4 activation, (^{4}He,x)	^{186}W	28.43	~6 mb at 43 MeV	[17]
	Proton activation, (p,α)	^{189}Os	16.15	~11 mb at 22 MeV	[25]
	Proton activation, (p,3nα)	^{192}Os	40.78	~80 mb at 24 MeV	[20]
Accelerator	Spallation reaction, ^{208}Pb+p	^{208}Pb	52.4	n.a.	[18]
	Spallation reaction, ^{197}Au+p	^{197}Au	100	n.a.	[19]

n.a.= not applicable

A detailed study on the excitation functions of ^{nat}W(d,x) and ^{nat}W(^{3}He,x) reactions were performed to optimize the parameters for the production of NCA ^{186}Re by using an external beam line of the AVF-930 cyclotron of the National Institute of Radiological Sciences, Japan. While the experimental findings of ^{nat}W(d,x) reactions has already been published [26], the data analysis for the ^{nat}W(^{3}He,x) reactions is in progress. Furthermore, since no earlier studies are available for the ^{nat}W(^{3}He,x) reactions, the measured data may find significance in many perspectives. Among the various studied reactions, although ^{186}W(d,2n)^{186}Re shows four times higher cross sections than that of ^{186}W(p,n)^{186}Re [26], both of them are promising and selected for this evaluation study because of

their consistency with the available facilities, since no high energy proton, neutron or α beams are required. The existing literatures of ^{186}W(p,n)^{186}Re and ^{186}W(d,2n)^{186}Re reactions cross-sections show a considerable variation in this evaluation aimed at obtaining accurate values of production cross sections for ^{186}Re radionuclide in NCA form. As a part of the CRP, a practical approach of nuclear data evaluation has been adopted considering only the experimental parameters, nuclide decay data etc. but not any other external parameters or hypothesis. The use of the SOK code, which works based on the least squares technique, is very effective to remove the existing discrepancies among the experiments and finally produce recommended cross sections together with a covariance matrix. The produced dataset is significant for end-users. Moreover, the estimated covariance matrices obtained in this evaluation help to improve the accuracy of the obtained data. Since the TENDL data showed a clear discrepancy with the present work and also with the available literature, the evaluated data might be helpful to improve the predicting capability of the widely used model code TALYS; knowledge of the underlying uncertainties in evaluated nuclear data, i.e. covariances, is useful to improve the accuracy of nuclear data. Details on the evaluation study has already been published [27]. The evaluated cross sections of ^{186}W(p,n)^{186}Re and ^{186}W(d,2n)^{186}Re reactions in comparison to the other reported data are shown in Fig. 11 and 12, respectively.

In respect to the experimental study of ^{nat}W(^{3}He,x) reactions, production cross sections for the ^{nat}W(^{3}He,x)$^{181,182\ m,182\ ,183,184m,184g,184g(cum),186g}$Re, ^{187}W and $^{182,\ 183,\ 185}$Os nuclear reactions were measured from the respective thresholds up to 55 MeV. The results were compared with the only data for ^{186}Re and ^{187}W available in literature and theoretical data extracted from the TENDL-2019 library and only a partial agreement among them was found. Independent cross sections for most of the radionuclides are reported here for the first time. Physical thick target yields for the investigated reaction products were deduced from the measured cross sections, but no comparison was made with the directly measured yields due to the absence of any such previous study. The deduced yield curves indicate that a batch yield of 13.5 GBq of ^{186}Re at EOB in NCA form could be obtained via 72 h irradiations of 28 MeV ^{3}He particle with a 100 µA beam current on a 100 µm thick metallic ^{186}W (100%) target.
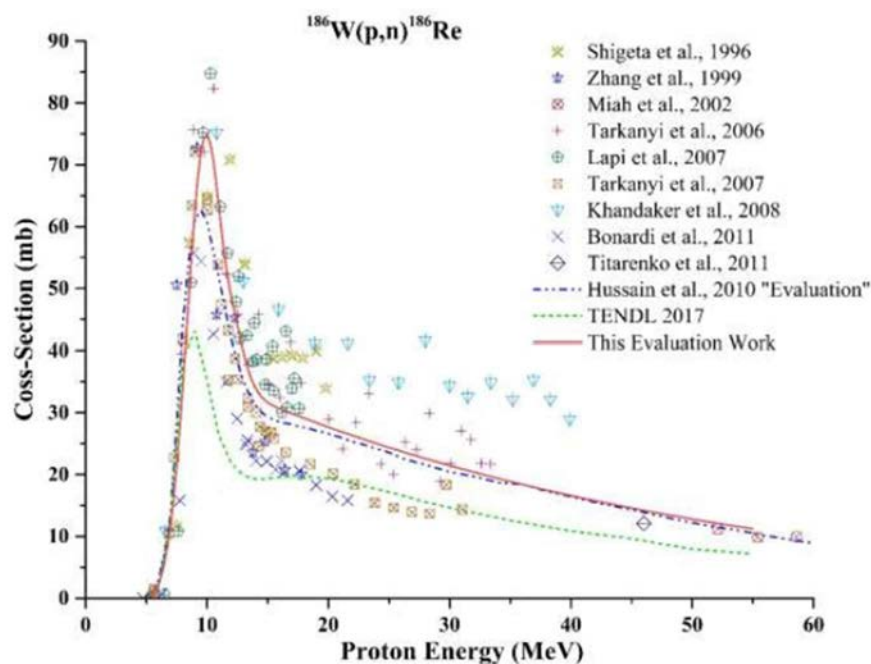
FIG. 11. Evaluated cross sections generated by SOK code combined with least squares method for the ^{186}W(p,n)^{186}Re reaction (Courtesy of Mr. Khandaker, University of Malaya, Malaysia).
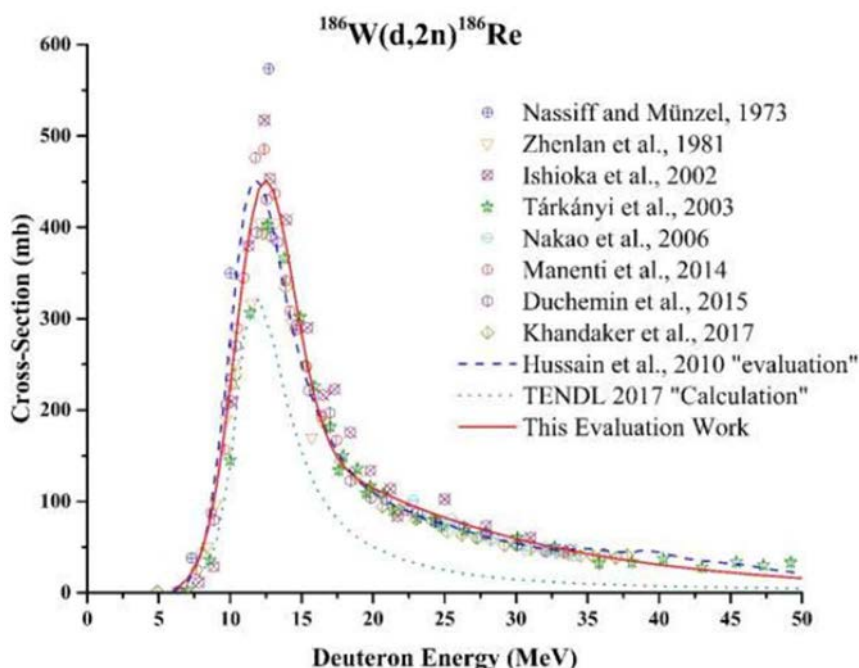
FIG. 12. *Evaluated cross sections generated by SOK code combined with least squares method for the $^{186}W(d,2n)^{186}Re$ reaction (Courtesy of Mr. Khandaker, University of Malaya, Malaysia).*

3.2. ^{186}Re PURIFICATION

Rhenium-186 was produced by deuteron induced reaction from an isotopically enriched ^{186}W target (natural abundance of ^{186}W = 28.6 atom%). Deuterons with an energy of approximately 20 MeV are favourable for production of ^{186}Re with considerable yield and acceptable radionuclidic purity [15, 16]. Production and radiochemical purification of ^{186}Re was carried out in an originally developed remote apparatus following the steps described below:

(a) Irradiate isotopically enriched ^{186}W powder prepared in the ceramic (SiC) target box with 20 MeV deuterons;
(b) Dissolve the activated ^{186}W in situ by loading of H_2O_2 + ammonium hydroxide solution;
(c) Transfer the crude ^{186}Re/^{186}W solution to hot cell through a tubing;
(d) Separate ^{186}Re from target matrix by using two chelating resins (TEVA and AnaLig Tc).

Results showed that approximately 87% of the activity of ^{186}Re produced was successfully recovered as the final product at a yield of 5.7±1.1 MBq (155±30 µCi)/µAh with >99.9% radiochemical purity of [^{186}Re]ReO$_4^-$. Total processing time was 4.5 h from the EOB, including target dissolving process of 2.5 h. Radionuclidic purity of ^{186}Re was 98.1% at 8 h from the EOB (in case of 2 h irradiation), which would be increased to 99.2% as the maximum by 92 h cooling time from the EOB. The reproducibility of the separation, particularly the AnaLig column is still being evaluated.

In another method, selective electrodeposition has been successfully utilized for radiochemical separation of radiorhenium from proton irradiated natural or isotopically enriched [^{186}W]WO$_3$ target. For preparation of the target, WO$_3$ powder both of natural isotopic composition and enriched (98.6% in ^{186}W) was pressed into a grooved aluminium holder to form a 10 mm diameter pellet with surface density of 11.53 mg/mm^2. The aluminium holder was covered with a 9.43 mg/cm^2 thick copper foil used as beam monitor and then fixed on the water-cooled target block. The irradiation was carried out using an incident proton beam of 12 MeV, with average beam intensity of 180 nA for 60 h. After

the end of irradiation, the target was cooled for 6 h, in order to allow the decay of short lived radionuclides. Subsequently, the target was dissolved in 10 mL of 4 M NaOH solution with few drops of H_2O_2. A small aliquot of the target solution was withdrawn, and its γ ray spectra were recorded using an HPGe detector coupled with MCA after appropriate dilution.

The radiochemical separation process involved selective electrodeposition of Re radioisotopes (indicated as *Re) from the radioactive solution obtained after radiochemical processing. The radioactive solution was directly transferred to the electrochemical cell and used as the electrolyte. A schematic diagram of the electrochemical cell is given in Fig. 13. The electrodes used were made of high purity platinum wires. The electrochemical cell consisted of a glass vial (24 × 40 mm, 20 mm ID) and a teflon cap. The electrodes (length 50 mm, diameter 1.5 mm) were fitted 5 mm apart on the teflon cap. The teflon cap and the electrodes were fitted on the mouth of the glass vial. The platinum electrodes were adjusted parallel to each other, connected to the power supply using small screws embedded into the teflon cap which were in contact with the electrode. A provision was supplied for passing gas through a glass tube, dipped into the electrolysis solution. A small hole (~2.5 mm) was opened in the teflon cap for venting off any gases, that may be formed. The effect of applied potential on electrodeposition of *Re was studied by measuring the percentage deposition of *Re as a function of voltage, when electrodeposition was performed at pH14. Experiments were then performed to ascertain the minimum time required for quantitative electrodeposition at optimum applied potential. After the electrolysis under optimized conditions, the electrodes were removed from the cell while maintaining the potential. It was turned off after removal of the electrodes from the solution. The cathode containing the electrodeposited *Re was then transferred to another narrow electrolytic cell containing 1 mL of 0.9% NaCl (saline) solution as the electrolyte. The polarity of the electrode was reversed, and a potential of 20 V was applied for 30 s leading to dissolution of *Re deposit in saline solution.
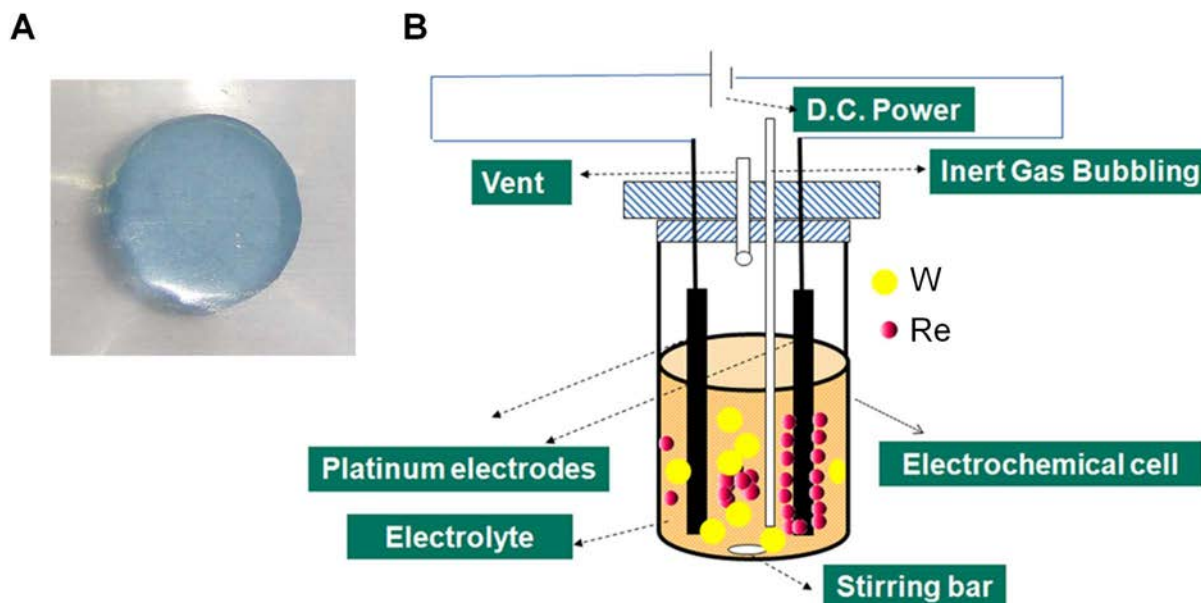
FIG. 13. (a) Pelletized natural tungsten oxide target prepared for irradiation, (b) schematic diagram of the set up for electrochemical separation (not drawn to scale) (Courtesy of Mr. Chakraborty, Bhabha Atomic Research Centre, India).

It was found that the maximum electrodeposition of *Re was achieved at an applied potential of 7 V. Also, a minimum of 30 min of electrolysis was required to achieve maximum electrodeposition yield. After electrodeposition, *Re could be retrieved in 1 mL of saline solution.

```
        Tungsten enriched target preparation 186W
                           │
                           ▼
            Irradiation (16 MeV, 150 µA protons)
                           │
                           ▼
        Target dissolution (Heating, H2O2, NaOH)
                           │
                           ▼
                      Evaporation
                           │
                           ▼
               Acid addition (0.1M HNO3)

TEVA Cartridge preconditioning
       1-HNO3
       2-H2O          ──►  Loading 186Re, 186W  ──►  186W for recovery
       3- HNO3 (0. 1M)
                           │                              ▲
                           ▼                              │
               Cartridge rinsing by HNO3 1M  ────────────┘
                           │
                           ▼
                186Re Elution HNO3 8M
```
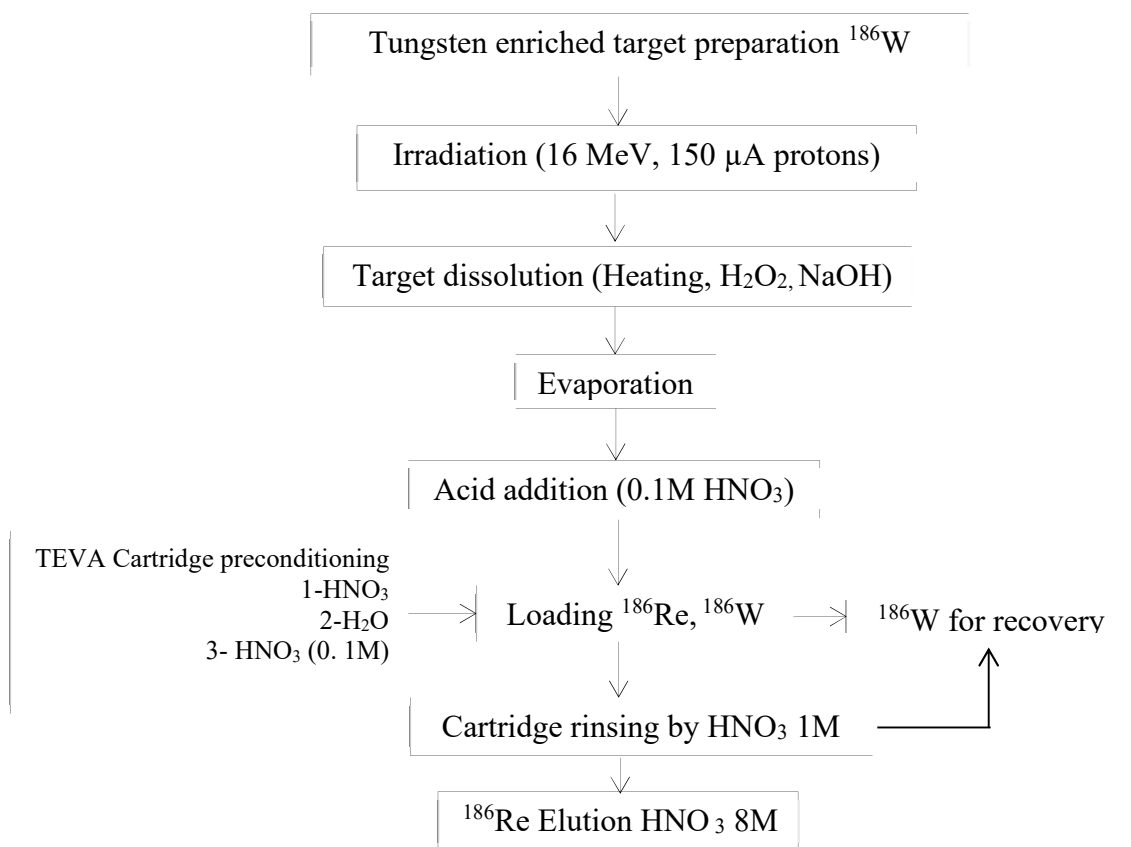
FIG. 14. Flow chart for production and radiochemical separation of ^{186}Re (Courtesy of Mr. Al Rayyes, Atomic Energy Commission of Syria, Syria)

Rhenium-186 was also produced by proton irradiations on WO_3 target carried out using a 30 MeV cyclotron. Production runs were conducted at 15 MeV proton beam of 150 µA intensity. The irradiation times were approximately 4 h. The target was 500 µm thick fixed on copper target holder. The back side of the copper target holder was cooled with a high speed stream of deionized water flowing through the irradiation station. The irradiated tungsten target was dissolved by hydrogen peroxide 30% and 1M NaOH, using a homemade system. The resulting solution was evaporated to dryness then the residue containing ^{186}W and ^{186}Re was re-dissolved using 0.1M nitric acid. This solution was loaded on a preconditioned TEVA cartridge. All ^{186}Re was retained by TEVA cartridge after rinsing the cartridge by 1 M nitric acid. [^{186}Re]ReO$_4^-$ was eluted from the TEVA cartridge with 8M HNO_3. The resulting solution was evaporated to dryness, then dissolved in 0.9% sodium chloride for injection and 2 drops of hydrogen peroxide 30% were added. Figure 14 shows the flow chart for production and radiochemical separation of ^{186}Re.

3.3. ^{186}Re QUALITY CONTROL

3.3.1. Radionuclidic purity

Yield and radionuclidic purity measurements were carried out using a pre-calibrated HPGe detector coupled to MCA. The γ ray spectrum of the solution of irradiated target before and after radiochemical purification by electrochemical route is given in Fig. 15 (a) and (b). When a WO_3 target of natural isotopic composition was used, the γ ray spectrum [Fig. 15(a)] showed the presence of ^{181}Re, ^{182m}Re, ^{182}Re, ^{183}Re, ^{184}Re, ^{187}W and ^{183}Ta, in addition to ^{186}Re. Peaks corresponding to ^{187}W and ^{183}Ta were not visible in the γ spectrum of the separated product after electrochemical separation [Fig. 15 (b)].

Similarly, when radiochemical purification was carried out using a TEVA cartridge, the γ spectra of the solution before and after purification were recorded (Fig. 16 (a) and (b)). The spectra of irradiated target solution before loading on TEVA cartridge showed the presence of radioisotopes of rhenium, ^{181}W and added radiotracer ^{65}Zn. Since the spectra were recorded 24 h post end of irradiation, ^{181}W formed from the decay of ^{181}Re ($T_{1/2}$ = 20 h). The resulting solution was passed through the preconditioned TEVA cartridge and the cartridge was rinsed with 1M of HNO$_3$. This process resulted in near complete removal of ^{181}W and ^{65}Zn [Fig. 16 (b)].

Hence, it is evident that both the processes described above resulted in Re radioisotopes of > 99.9% radionuclidic purity.
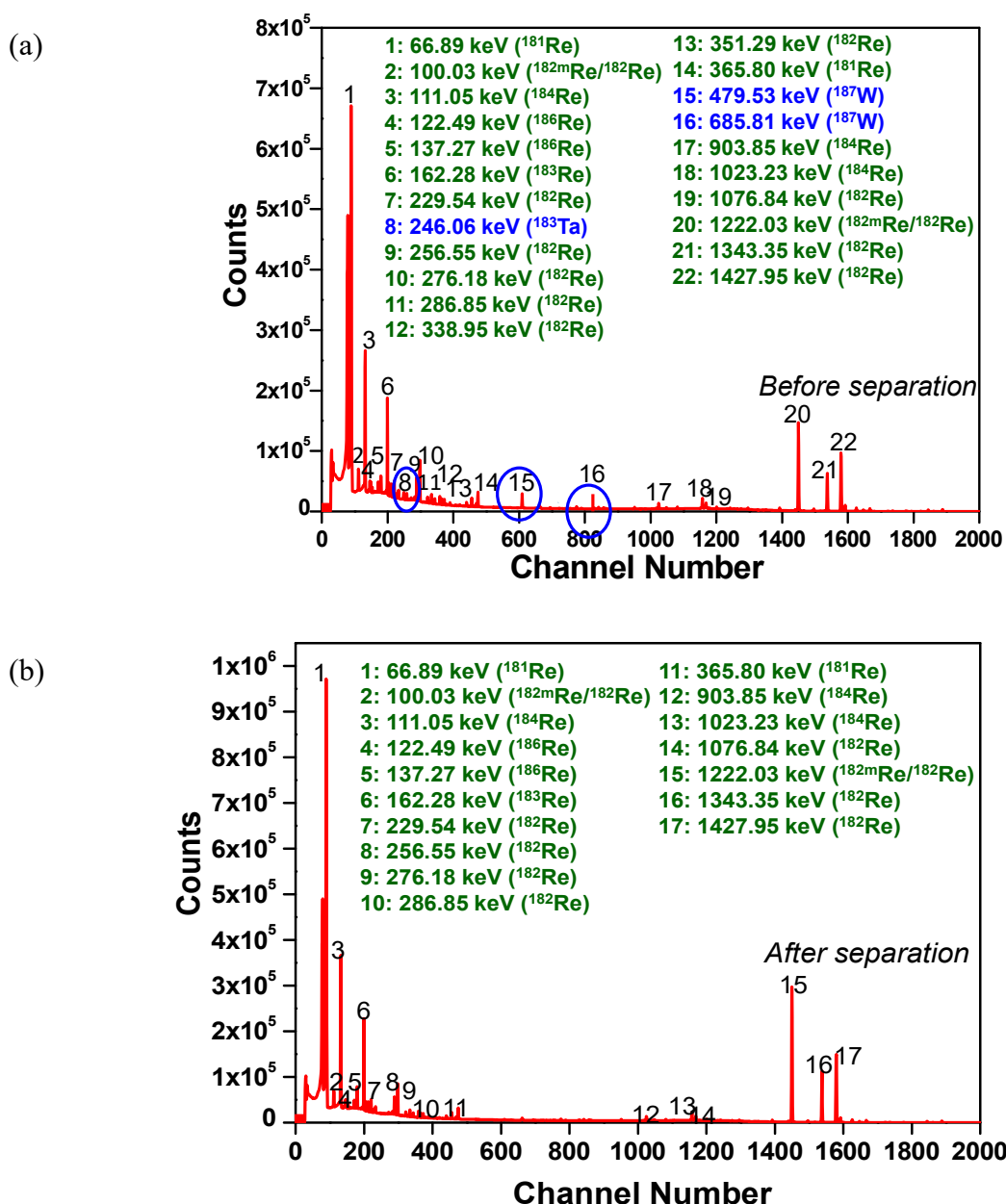
FIG. 15. γ ray spectrum of the solution (a) before and (b) after radiochemical separation of Re radioisotopes using electrochemical route and natural WO₃ as a target material (Courtesy of Mr. Chakraborty, Bhabha Atomic Research Centre, India).
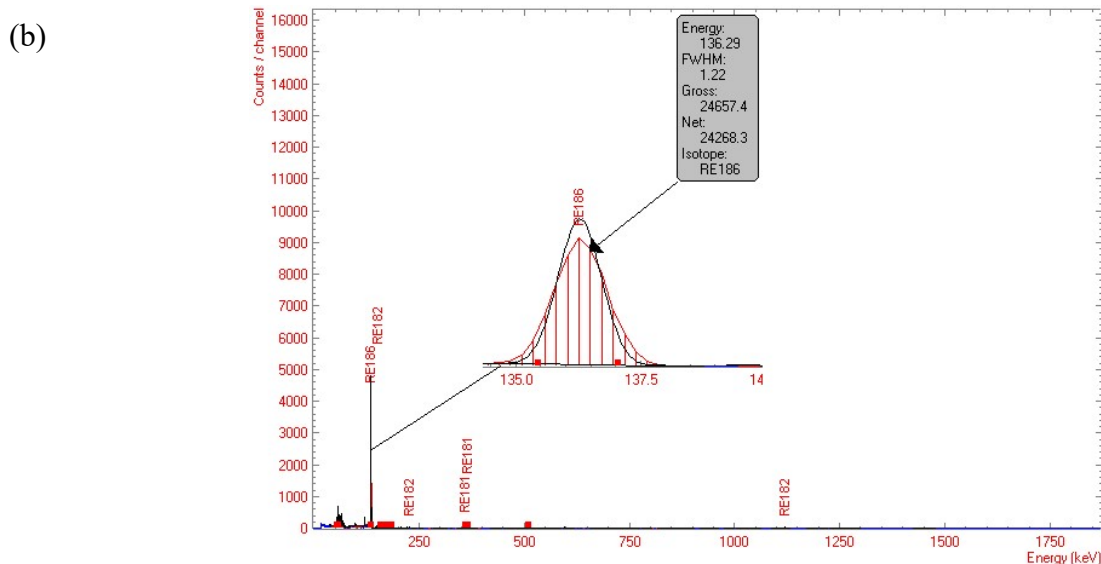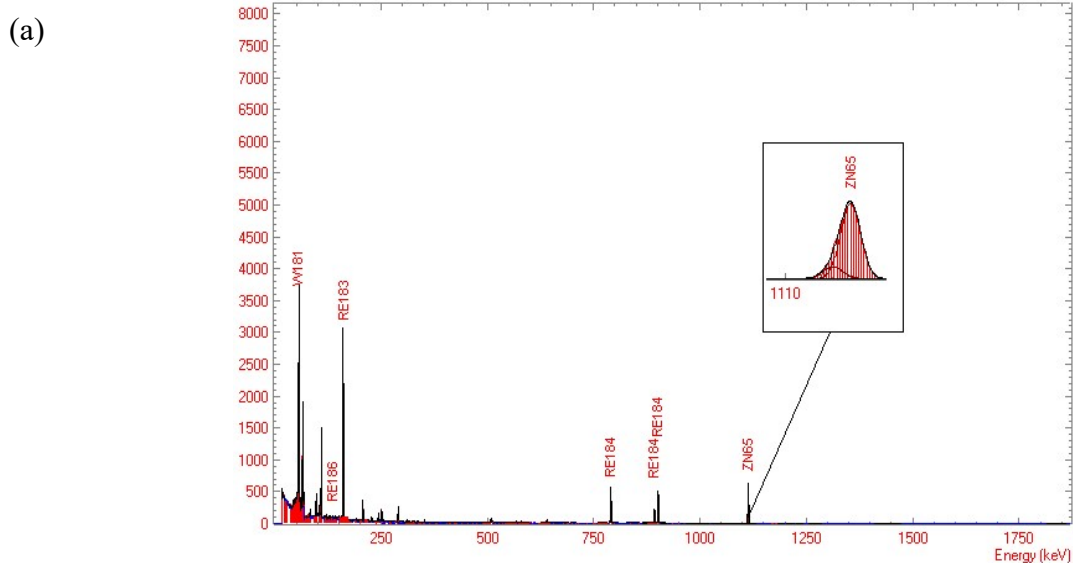
FIG. 16. γ ray spectrum of the solution (a) before and (b) after radiochemical separation of Re radioisotopes using TEVA cartridge when natural WO₃ used as target material (Courtesy of Mr. Al Rayyes, Atomic Energy Commission of Syria, Syria).

3.3.2. Radiochemical purity

To evaluate the radiochemical purity of Re in the form of ReO_4^-, 5 μL of test solution was applied on paper chromatographic strips (Whatman 12 cm×1 cm) at 1.5 cm from the lower end. The strips were developed in 0.9% saline. Subsequently, the paper strip was dried, cut in to 1 cm segments, placed in test tubes and counted in a NaI(Tl) scintillation counter. Radiochemical purity was found to be >98 %.

3.3.3. Chemical purity

In order to determine the level of other metallic impurities (mainly in the form of W) present in purified [186]Re solution, the samples were allowed to decay for 1 month and inductively coupled

plasma (ICP)–atomic emission spectroscopy analyses were carried out. Results indicated that the level of stable tungsten and rhenium isotopes was below detectable limit (< 0.01 µg/mL).

4. ^{47}Sc PRODUCTION AND RADIOCHEMISTRY

4.1. ^{47}Sc NUCLEAR DATA

Scandium-47 has a half-life of 3.35 d and decays by β$^-$ emission. Scandium-47 can be produced via different nuclear reactions using cyclotrons, nuclear reactors and electron linear accelerators. It is possible to produce ^{47}Sc directly or via decay of the parent ^{47}Ca radionuclide; this latter route requires a double chemical separation to extract ^{47}Sc from the ^{47}Ca/^{47}Sc generator. In case of direct ^{47}Sc production, particular attention should be given to the co-production of contaminant radionuclides, especially long lived Sc isotopes such as ^{44m}Sc, ^{46}Sc and ^{48}Sc, that cannot be chemically separated from the desired product. Additionally, ^{47}Sc via the ^{47}Ca/^{47}Sc generator may contain Sc isotopes generated by the decay of different Ca isotopes co-produced during the irradiation of the target material. This section presents nuclear data associated with the charged particles induced reactions that can be used with particle accelerators and the n-induced reactions feasible in reactors and linear accelerators.

4.1.1. Production of ^{47}Sc using accelerators

Several charged particle reactions for direct and indirect ^{47}Sc co-production can be induced on Ca, Ti and V target materials. To compare the different production routes, the expected yield of the main reaction as well as yields of the side reactions for radionuclidic impurities were calculated, applying the same irradiation parameters. The analysis includes a feasibility study of each reaction by including determination of:

— The expected yield of the reaction;
— The optimal bombarding energy window to minimize the production of the possible contaminating radionuclides;
— The required amount of target material and target thickness;
— The expected radio-contamination level;
— The expected maximum specific activity of ^{47}Sc.

The activity of all the radionuclides of interest (^{47}Sc, ^{47}Ca and ^{xx}Sc contaminants) was determined considering both direct and indirect production routes. Production of stable ^{45}Sc was also assessed for the indirect route. The decay production includes decay chains with maximum five elements (four decay steps). The activity of the main products and the total activity of the contaminating isotopes were calculated at EOB and after a certain cooling time. The cooling time was selected to be long enough to make the necessary chemical processing of the irradiated target and/or to reduce the amount of the co-produced contaminating radionuclides. For production routes of ^{47}Sc, a 24 h long irradiation with 1 eµA beam intensity was chosen with:

— 24 h cooling time to minimize the amount of other coproduced Sc radioisotopes, in case of direct routes;
— 3 h cooling time to separate ^{47}Ca from the irradiated target and additional 134 h cooling time to the first elution of the ^{47}Ca/^{47}Sc generator, in case of indirect routes.

For direct production routes, twelve charged particle induced reactions were studied:

(a) Direct reaction on Ti targets for proton and deuteron bombardment:

— ^{50}Ti(p,α)^{47}Sc;
— ^{49}Ti(p,^{3}He)^{47}Sc;
— ^{48}Ti(p,2p)^{47}Sc;
— ^{50}Ti(d,αn)^{47}Sc;
— ^{49}Ti(d,α)^{47}Sc;
— ^{48}Ti(d,^{3}He)^{47}Sc;
— ^{47}Ti(d,2p)^{47}Sc.

(b) Direct reaction on Ca targets for proton, deuteron and α particle bombardment:

— ^{48}Ca(p,2n)^{47}Sc;
— ^{48}Ca(d,3n)^{47}Sc;
— ^{46}Ca(d,n)^{47}Sc;
— ^{44}Ca(α,p)^{47}Sc.

(c) Direct reaction on V target for proton:

— ^{51}V(p,αp)^{47}Sc

For indirect production routes six charged particle induced reactions were studied:

(a) Indirect reaction on Ti targets for proton and deuteron bombardment:

— ^{50}Ti(p,p^{3}He)^{47}Ca →^{47}Sc;
— ^{49}Ti(p,3p)^{47}Ca → ^{47}Sc;
— ^{50}Ti(d,αp)^{47}Ca → ^{47}Sc.

(b) Indirect reaction on Ca targets for proton and deuteron bombardment:

— ^{48}Ca(p,d)^{47}Ca →^{47}Sc;
— ^{46}Ca(d,p)^{47}Ca →^{47}Sc;
— ^{48}Ca(d,t)^{47}Ca →^{47}Sc.

Production of ^{47}Sc on stable Ti and Ca isotopes requires enriched target material; therefore, a 98% enrichment level was assumed for each target isotope. Among all the reactions listed above, only the ^{nat}V targets do not require an enriched target. Table 7 reports the natural abundance of the target materials needed for ^{47}Sc production, as extracted from the NuDat 2.7 database [28]. The ^{48}Ti(γ,p)^{47}Sc reaction is discussed briefly in the discussion section of this publication as it is based on significantly different accelerator technology, but nevertheless warrants further separate investigation (i.e. electron-accelerators).

Most of the excitation functions of the nuclear reactions included in the calculations were taken from the TENDL-2017 data library available online [3]. Therefore, if available, evaluated experimental cross section data were used for the main reaction. Table 8 and Table 9 compare all direct and indirect production routes of ^{47}Sc, respectively. The most suitable reaction can be selected for every target

26

material and type of bombarding particle by considering additional parameters, including availability and cost of target material, required amount of activity of the [47]Sc radioisotope, and necessary target purification chemistry.

TABLE 7. NATURAL ABUNDANCE OF TARGET MATERIALS FOR [47]Sc PRODUCTION

Target	Abundance (%)
[51]V	99.750%
[50]Ti	5.18%
[49]Ti	5.41%
[48]Ti	73.72%
[48]Ca	0.187%
[46]Ca	0.004%
[44]Ca	2.09%

TABLE 8. COMPARISON OF DIRECT PRODUCTION ROUTES OF [47]Sc ON Ca, Ti, AND V TARGETS
(*24 h irradiation, 24 h cooling time, 1 eµA beam current*)

	E_{in} (MeV)	E_{out} (MeV)	Target (98%)	Target thickness (µm)	[47]Sc activity at EOB (MBq)	[47]Sc activity after cooling (MBq)	Activity of other Sc after cooling (MBq)	Radioisotopic Purity (%)
[50]Ti(p,α)[47]Sc	20	8	[50]Ti	1132	93	76	0.5	99
[49]Ti(p,[3]He)[47]Sc	40	28	[49]Ti	2262	580	472	353	57
[48]Ti(p,2p)[47]Sc	25	18	[48]Ti	922	69	56	26	68
[50]Ti(d,αn)[47]Sc	27	20	[50]Ti	581	341	278	24	92
[49]Ti(d,α)[47]Sc	12	3	[49]Ti	321	41	34	0.67	98
[48]Ti(d,[3]He)[47]Sc	44	34	[48]Ti	1214	800	651	315	67
[47]Ti(d,2p)[47]Sc	25	10	[47]Ti	993	292	237	246	49
[48]Ca(p,2n)[47]Sc	23	18	[48]Ca	1659	3518	2936	297	91
[48]Ca(d,3n)[47]Sc	29	24	[48]Ca	1184	2807	2348	630	79
[46]Ca(d,n)[47]Sc	5	2	[46]Ca	164	168	137	0.70	99
[44]Ca(α,p)[47]Sc	17.8	7	[44]Ca	220	50	41	0.19	≈100
[51]V(p,αp)[47]Sc	30	20	[51]V (99.75%)	1127	25	20	0.004	≈100

As shown in Table 9, the reactions providing the highest [47]Sc yield are [48]Ca(p,2n)[47]Sc and [48]Ca(d,3n)[47]Sc. On the other hand, the reactions with the lowest predicted contamination level are [50]Ti(p,α)[47]Sc, [46]Ca(d,n)[47]Sc, [44]Ca(α,p)[47]Sc and [51]V(p,αp)[47]Sc. The [48]Ca(p,2n)[47]Sc reaction leads to an experimental [47]Sc radionuclidic purity of only 87% for the 24→17 MeV energy range [29]; however, while the expensive enriched [48]Ca material makes this route challenging GBq quantities of [47]Sc may be achievable. The advantage of the [44]Ca(α,p)[47]Sc reaction lies in the short range of α projectiles in Ca target, allowing the use of a relatively small amount of [44]Ca target material for small scale studies with [47]Sc. For example, it is reported that 200 mg of [[44]Ca]CaO prepared in a diameter of 10 mm would give a yield of approximately 11 MBq at 10 eµA for 2 h irradiation at the end of preparation (approximately 1.5 h from the EOB) in the energy range of 28 → 0 MeV [30].

As reported in Table 9, using the 17.8–7 MeV energy window for α particles, the expected total radiocontamination is less than 0.5%. This is possible by selecting an energy window where the contaminating ^{46}Sc is not produced. In fact, the maximum of the excitation function for the ^{44}Ca(α,p)^{47}Sc reaction is near the threshold energy of the ^{44}Ca(α,d)^{46}Sc reaction; thus, in principle, this reaction can provide pure ^{47}Ca. The actual purity of the ^{47}Sc product depends on the composition of the enriched ^{44}Ca target material; preferably low amounts of ^{43}Ca should be present to minimize the amount of co-produced ^{46}Sc.

The ^{51}V(p,αp)^{47}Sc reaction can be used with ^{nat}V targets and, although it provides a quite low ^{47}Sc yield, it offers great advantage. It does not require expensive enriched target material since the vanadium is inexpensive and commercially available in metallic form. By setting the proton energy window at 30 MeV, i.e. below the threshold of the (p,α2p) reaction to avoid the ^{46}Sc contamination, this route can be used to produce small amounts of pure ^{47}Sc. Thick target yield based on experimental data were calculated at the EOB for the 30 → 19 MeV energy range, showing that the production of ^{47}Sc is 31 MBq/µA and 82 MBq/µA for 24 h and 80 h irradiation runs, respectively, while the co-production of ^{46}Sc can be considered nearly negligible, i.e. respectively 0.01 MBq 0.03 MBq per µA [31].

TABLE 9. COMPARISON OF INDIRECT PRODUCTION ROUTES OF ^{47}Sc ON Ca AND Ti TARGETS
(24 h irradiation, 3+134 h cooling time, 1 µA beam current)

	E_{in} (MeV)	E_{out} (MeV)	Target (98%)	Target thickness (µm)	^{47}Ca activity at EOB (MBq)	^{47}Sc activity after elution (MBq)	Atom ratio ^{47}Sc/^{45}Sc
^{50}Ti(p,p3He)^{47}Ca→^{47}Sc	80	40	^{50}Ti	6764	28.1	11.7	1.57
^{49}Ti(p,3p)^{47}Ca→^{47}Sc	80	40	^{49}Ti	6764	13.4	5.6	0.58
^{50}Ti(d,αp)^{47}Ca→^{47}Sc	35	15	^{50}Ti	1733	4.02	1.68	79.1
^{46}Ca(d,p)^{47}Ca→^{47}Sc	14	5	^{46}Ca	981	89	37.1	556
^{48}Ca(d,t)^{47}Ca→^{47}Sc	30	13	^{48}Ca	3416	682	284	806
^{48}Ca(d,t)^{47}Ca→^{47}Sc	50	13	^{48}Ca	9918	4315	1798	79
^{48}Ca(p,d)^{47}Ca→^{47}Sc	30	11	^{48}Ca	6270	1691	705	724
^{48}Ca(p,d)^{47}Ca→^{47}Sc	50	11	^{48}Ca	17561	5800	2418	35

As shown in Table 9, the reactions providing the highest ^{47}Sc activity are ^{48}Ca(d,t)^{47}Ca→^{47}Sc, ^{48}Ca(p,d)^{47}Ca→^{47}Sc and ^{46}Ca(d,p)^{47}Ca→^{47}Sc. In case of indirect production of ^{47}Sc on Ca, the only Sc contamination is the ^{45}Sc from decay of ^{45}Ca. Since ^{45}Sc is stable, it may only affect the isotopic purity and the specific activity of the final product from a theoretical perspective (i.e. not considering any potential stable Sc or other competing metals introduced through chemical processing). The ^{48}Ca(p,d)^{47}Ca→^{47}Sc reaction was studied up to 60 MeV by using ^{nat}CaCO$_3$ targets and scaling the results to 69% enriched [^{48}Ca]CaCO$_3$ [29]. However, this route has not been experimentally widely investigated due to the prohibitive cost of the enriched ^{48}Ca material.

4.1.2. Production of ^{47}Sc by nuclear reactors

Scandium-47 can be produced in nuclear reactors via the:

— Direct reaction ^{47}Ti(n,p)^{47}Sc with fast neutrons flux (E > 1 MeV);
— Indirect reaction ^{46}Ca(n,γ)^{47}Ca→^{47}Sc with thermal neutron fluxes.

Due to the presence of different isotopes in the target with different abundances, many radiocontaminants will be generated upon neutron irradiation of calcium or titanium. Among these, ^{46}Sc and ^{48}Sc radionuclides are the most noteworthy, due to their longer half-lives and high energetic γ emissions. The expected yield of ^{47}Sc estimated for 10 mg of 66% enriched ^{47}Ti, irradiated for 143 h with $3{\times}10^{13}$ neutron/cm^{2}s is approximately 31 MBq.

The cross section of the ^{46}Ca(n,γ)^{47}Ca reaction is 0.74 barn for thermal neutrons, which is relatively high, but ^{46}Ca natural abundance is extremely low (0.004%). Hence, to obtain significant yields of ^{47}Ca, an enriched ^{46}Ca target must be used, which is rather, perhaps prohibitively expensive. Irradiation of 1 g natural CaCO$_3$ at a thermal neutron flux of 1.8×10^{14} neutron/cm^{2}s in the Egyptian Second Research Reactor (ETRR-2) gave 0.84 MBq of ^{47}Sc [32]. When 48.5 mg of 5.2% enriched [^{46}Ca]CaCO$_3$ (equivalent to 0.97 mg of ^{46}Ca) were irradiated at the Maria reactor (Poland) for 150 h with $1.2{\times}10^{14}$ neutron/cm^{2}s, the measured activity of ^{47}Ca at EOB was around 700 MBq [33]. On irradiation of ~100 mg of 10% [^{46}Ca]CaCO$_3$ target at a flux of 1×10^{14} neutron/cm^{2}s for 14 days in the Dhruva research reactor, India, the activity of ^{47}Sc after radiochemical processing was 2.9 GBq [34]. A comparative study of the ^{47}Ti(n,p)^{47}Sc and ^{46}Ca(n,γ)^{47}Ca→^{47}Sc routes was carried out to determine the ^{47}Sc yield and radionuclidic purity of each route [35]. The ^{46}Ca(n,γ)^{47}Ca reaction provided higher quantities of a radioisotopically pure product, i.e. 1.5 GBq of ^{47}Sc (> 99.99% pure). Even if the high price of enriched ^{46}Ca represents a drawback, this reaction was considered favourable in respect to the ^{47}Ti production route with fast neutrons, which provided 1.8–10.0 MBq ^{47}Sc/mg of ^{47}Ti (at the flux of 10^{13}neutron/cm^{2}s) and ^{47}Sc radioisotopic purity with reduced (99.95–88.5%).

4.2. ^{47}Sc TARGET PREPARATION

The production of radionuclides can be carried out using various target forms such as solid, liquid or gas. Accordingly, competence in engineering, chemistry, and material sciences are essential in the choice of a specific target (solid, liquid, or gas target). There are various forms of solid targets such as metallic foil/coin, metallic powder, or oxide forms.

There are some important considerations that impact the choice of target material, including the following:

(a) The atomic density of the target species in the target material (for example, a solid or liquid might provide higher atomic densities than a gas and thus produce greater quantities of the desired product);
(b) The cross section of the desired target atoms for the particular nuclear reaction of interest (for example, a small cross section may require higher target density, often using a solid or liquid target over a gas);
(c) The purity of the target material (some target materials may contain species that produce undesired radionuclides that might be difficult to separate from the desired species);
(d) The number of isotopes in the target material; the fewer number the better (undesired radioactivity of the target materials after irradiation as a consequence of generating high radiation levels of some potential target materials).

4.2.1. Calcium targets for the production of ^{47}Sc

So far, only three methods for obtaining ^{47}Sc on calcium targets have been widely developed: neutron activation of ^{46}Ca and proton and γ irradiation of ^{48}Ca. In the neutron irradiation of a ^{46}Ca target, ^{47}Ca is produced which then decays to ^{47}Sc via $^{46}Ca + n \rightarrow {}^{47}Ca \rightarrow {}^{47}Sc$.

For neutron irradiation of enriched ^{46}Ca, standard procedures for reactor target preparation are used. In a method developed by Pawlak et al. the target material, 5% enriched [^{46}Ca]CaCO$_3$, was sealed in double quartz ampoules [33]. After irradiation, the outer ampoule was cut with a diamond saw. The inner ampoule had a thinner tip which could be easily broken, so that the powder could be poured and dissolved in the hydrochloric acid. In other studies, highly enriched [^{46}Ca]CaCO$_3$ (83.09%) was used [35]. Alternatively, irradiation of a ^{46}Ca target (dried nitrate, 31.7% enrichment of ^{46}Ca) was carried out for 3.94 d in a thermal neutron flux of 1.5×10^{15} n cm^{-2} s^{-1} at the high-flux reactor of Institut Laue Langevin in Grenoble, France [36]. In this method, Siwowska et al. optimized the production and separation processes of ^{47}Sc with the use of [^{46}Ca]CaO (^{46}Ca, 5% enrichment) targets instead of [^{46}Ca]CaCO$_3$ or Ca(NO$_3$)$_2$ targets [36]. The targets were also irradiated in quartz ampoule in high flux reactor at the Institut Laue Langevin.

For cyclotron production of ^{47}Sc by proton irradiation of a ^{48}Ca target, ^{47}Sc is produced directly via the (p,2n) nuclear reaction, but contains also high impurities of ^{48}Sc and ^{46}Sc. In the second method, ^{47}Ca produced via the (p,d) reaction is separated from ^{46}Sc and ^{48}Sc and then decays over 5.6 days to ^{47}Sc. Up to now, only production yield of ^{47}Sc and ^{48}Sc radionuclides on CaCO$_3$ targets with natural isotopic composition [29] and enriched targets were measured as function of proton energy in the range of 60→0 MeV using activation method on stacks. The stack consisted of thin metallic foils with natural isotopic composition interleaved with CaCO$_3$ targets. The stack was assembled from six groups of Al-Cu-CaCO$_3$ and five groups of Al-Cu-Ti-CaCO$_3$.

4.2.2. Titanium targets for the production of ^{47}Sc

In a cyclotron, the four most investigated proton induced reactions that can be used to produce ^{47}Sc on stable isotopes of Ti are: ^{48}Ti(p,2p)^{47}Sc, ^{49}Ti(p,^{3}He)^{47}Sc, ^{49}Ti(p,3p)^{47}Ca→^{47}Sc and ^{50}Ti(p,α)^{47}Sc. Additionally, ^{47}Sc can be produced by α particle activation of titanium target through the (α,αpxn) nuclear reaction. Each reaction requires highly enriched target material to prevent or minimize the amount of unwanted contamination of the other Sc radionuclides.

Titanium targets can be made from Ti foil or by pressing TiO$_2$ powder into a pellet. Different types of targetry systems have been designed and manufactured for production of ^{47}Sc from the irradiation of Ti targets by cyclotrons.

One of the targetry systems includes an aluminium canister consisting of the target foil or pellet and target carrier (known as the shuttle), holding the canister (Fig. 17). The advantage of this design is the ability to move the canister to the cyclotron beam line and to the hot cell by a pneumatic transfer system. In this system, the Ti target was prepared by pressing the TiO$_2$ powder as a pellet and placing it into an aluminium canister (Fig. 18). The Ti target in the aluminium canister was placed in front of an aluminium target holder for irradiation. During irradiation, the target was cooled by water from the rear side (Fig. 19). The heat transfer and temperature distribution on the target was investigated based on a computational fluid dynamics. The modelled temperature distribution on the layer of Ti showed that the developed targetry system can be irradiated with the 30 MeV proton beam at a current of up to 50 μA and a water flow rate of 45 L/min.
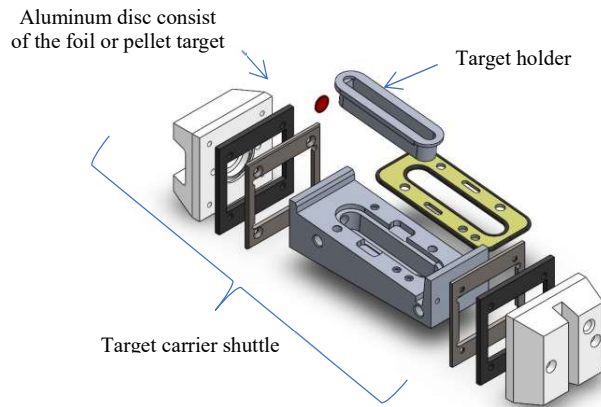
FIG. 17. Targetry system for irradiation of Ti and shuttle to facilitate the transfer of the target (Courtesy of Mr. Aboudzadeh-Rovais, Nuclear Science and technology Research Institute, Iran).
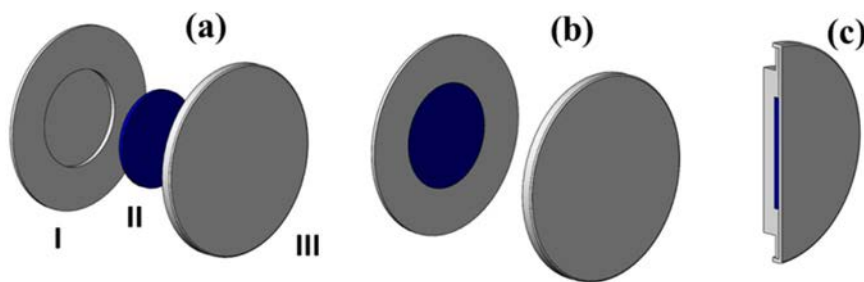
FIG. 18. Scheme of the (a) target canister consisting of I; the aluminium plate, II; titanium target and III; aluminium "cap", (b) titanium target put into the aluminium plate (c) cross-sectional cutting of target canister (Courtesy of Mr. Aboudzadeh-Rovais, Nuclear Science and technology Research Institute, Iran).
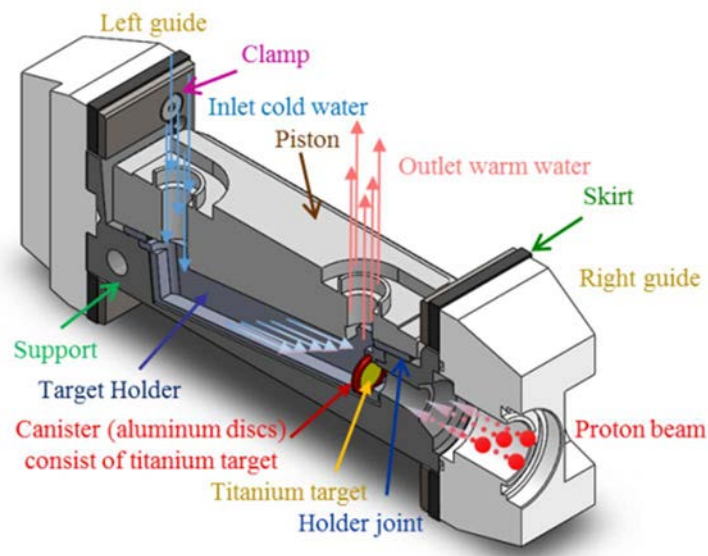
FIG. 19. Parts of the shuttle to facilitate the transfer of the encapsulated target (Courtesy of Mr. Aboudzadeh-Rovais, Nuclear Science and technology Research Institute, Iran).

In another targetry system, natural Ti foils were irradiated using the target holder shown in Fig. 20. The target foils are placed in a coin style target system with water cooling on the back and helium cooling on the front.
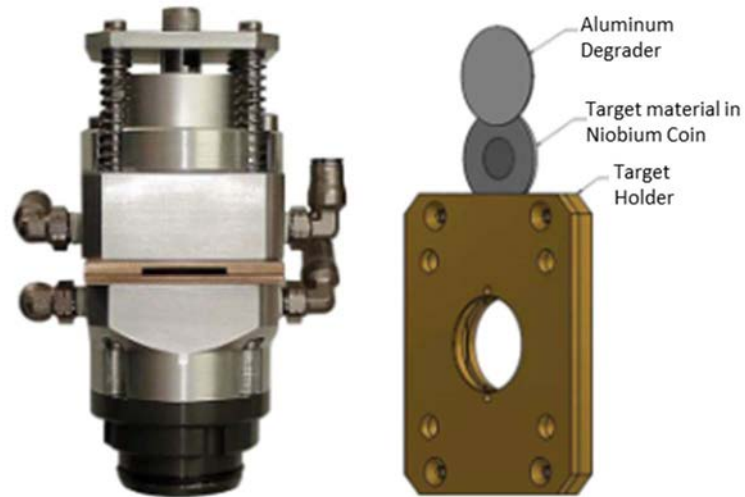
FIG. 20. Coin style target for foil, powder or electroplated irradiations (Courtesy of Ms. Lapi, University of Alabama, USA).

In this system, a niobium coin with a small divot in the centre to accommodate the foils was used. A photograph of an irradiated coin and target foil is shown in Fig. 21. Irradiations of 30 µA using proton energies of 18–24 MeV have been accomplished with this target configuration.
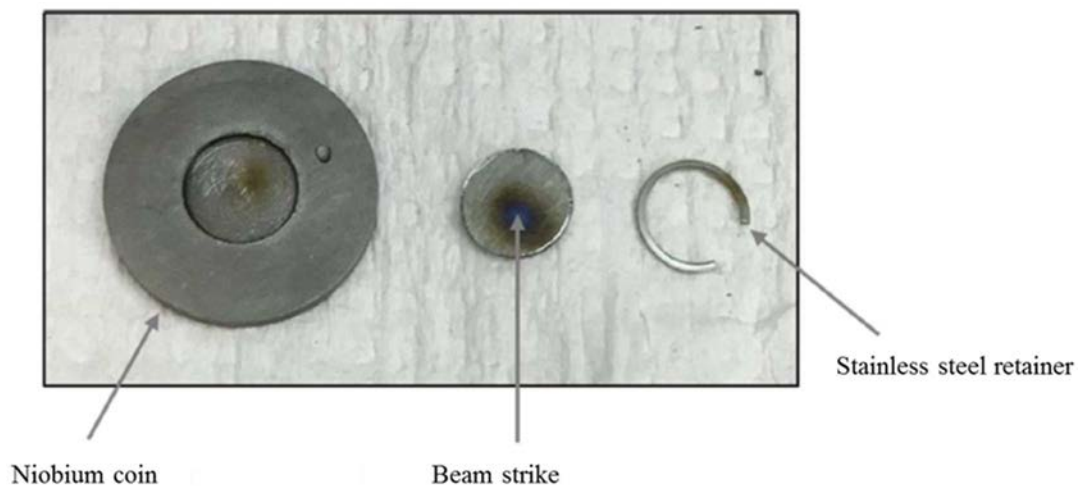
FIG. 21. Target assembly for irradiation of titanium foils (Courtesy of Ms. Lapi, University of Alabama, USA).

Another developed coin target system consisted of magnetized target halves which could accommodate titanium dioxide powder sealed with an O-ring. This target system is shown in Fig. 22.

FIG. 22. Powder titanium oxide target folder (Courtesy of Ms. Lapi, University of Alabama, USA).

Irradiation studies with this target system demonstrated that beam currents up to 40 µA could be achieved with no loss of target material integrity.

4.2.3. Vanadium targets for the production of ^{47}Sc

As mentioned in the previous section regarding the nuclear data for ^{47}Sc production, the advantage of the ^{51}V(p,αp)^{47}Sc reaction is that it can be achieved with ^{nat}V targets (^{51}V: 99.750%, ^{50}V: 0.250%). ^{nat}V material is readily commercially available in metallic form with high purity (99.8%) and several geometric characteristics (thickness and dimensions of the foil).

4.3. SEPARATION CHEMISTRY OF ^{47}Sc

4.3.1. Purification of ^{47}Sc From Ca targets

Production of ^{47}Sc with the high purity required for medical applications requires the development of efficient methods of separating trace amounts of scandium from bulk amounts of calcium target material.

The methods previously developed for ^{43}Sc and ^{44}Sc production were tested by Walczak et al. [37] for possible application in separation of ^{47}Sc from natural and enriched ^{46}Ca targets. First, the method based on separation with chelating resins reported by Krajewski et al. starting with dissolution of the target in 1M HCl and adsorption of scandium radionuclides on chelating ion exchange resin Chelex 100 was tested [38]. The scandium radionuclides were eluted from Chelex-100 column with 1M HCl in 0.5 mL fractions. Gizawy et al. further optimized the separation yield of ^{47}Sc obtained by Krajewski et al. to increase the recovery to 95 ± 0.87 % using 1M HNO$_3$ solution, where the sorption behaviour of ^{47}Sc in HNO$_3$ solution showed high affinity towards Chelex-100 compared with HCl solution [32] . In another method, described by Valdovinos et al., the irradiated ^{nat}CaCO$_3$ target was dissolved in 1 mL of 9M HCl solution [39]. The dissolved target solution was passed through a column containing UTEVA resin. To isolate scandium from the target material Ca^{2+} cations the column was rinsed with 9M HCl and the scandium radioisotopes were eluted with a 400 µL portion of H$_2$O. In another method described by Minegishi et al. the calcium target was dissolved in 0.5M HCl and subsequently pH adjusted with 25% NH$_3$ solution to pH10 [30]. The obtained Sc solution was then passed through a 0.2 µm filter (Whatman) to trap Sc radioisotopes; once trapped on the filter they were then eluted with 0.5M HCl. The acidity of ^{47}Sc solutions obtained by precipitation and separation by Chelex and UTEVA resins was too high for direct use for radiolabelling of peptide (pH for these radiolabelling reactions should be within 4.0 to 4.5 range) and therefore the collected eluate was adsorbed on a column filled with DOWEX 50WX4 cation exchange resin. The final elution of ^{44}Sc was performed using 1.5 mL 1M ammonium acetate aq. solution (pH4.5). Pawlak et al., in addition to the separation methods listed above, tested two methods originally developed for ^{44}Sc separation from calcium targets [33]. In the first method described by Domnanich et al., ^{47}Sc was adsorbed on DGA resin and eluted with 0.05M HCl [35, 40]. The final eluent can be used directly for labelling of DOTA (1,4,710-tetraazacyclododecane-1,4,7,10-tetraacetic acid) bioconjugates. In the second method, an extraction chromatography method with hydroxamate resin reported by Severin et al. for isolation of ^{44g}Sc from metal calcium target was used to isolate ^{47}Sc from CaCO$_3$ target [41]. From those evaluated separation methods, the highest ^{47}Sc recovery (> 90%) was achieved by applying a precipitation method and the application of DGA resin. Additionally, the radiolabelling yield of DOTA-TATE was the highest (>95 %) when ^{47}Sc obtained by these methods was used.

In addition to the presented methods, two new approaches have been designed specifically for the separation of ^{47}Sc from calcium targets. The first one was reported by Chakravarty et al. who applied

selective reduction of Ca^{2+} ion and preferential transfer of Ca metal onto a mercury cathode by the application of controlled potential [34]. ^{47}Sc was obtained with >80% yield and met all the requirements for clinical use. The second approach was reported by Gizawy et al. where the separation of ^{47}Sc from irradiated Ca target was achieved via P(AAm-AA)/MWC NTs) composite column resulting an elution efficiency of 80 ± 1.5 % for ^{47}Sc using 1 M HNO_3 [32]. The eluted final ^{47}Sc solution had significant chemical (Ca and Ti<0.05 ppm) and radionuclidic (>99%) purity.

4.3.2. Purification of ^{47}Sc From Ti targets

While for ^{47}Sc production from calcium targets the proposed separation methods are relatively simple and fast [29], in the case of titanium targets the procedures are longer, mainly due to the time consuming dissolution and evaporation steps associated with dissolving titanium, in particular in the TiO_2 form. A fast way to dissolve titanium involves the use of hydrofluoric acid (HF) which comes with some significant safety concerns and accordingly requires the employment of chemically HF resistant material (plastic or Teflon®) [42]. Different dissolution methods have been investigated with the aim of avoiding use of HF ranging from hot concentrated hydrochloric or reflux sulfuric acid, to mixtures of hot sulfuric acid containing ammonium sulphate. An in situ HF production, based on the use of a mixture of concentrated HCl and NH_4HF_2, has been found to be the most rapid technique able to dissolve titanium both in metal and oxide form in few minutes (<5 min) [43]. Post-dissolution treatment such as: evaporation, dilution, pH adjustment or addition of few drops of H_2O_2 to convert Ti (III) to Ti (IV), have been adopted in order to convert the chemical species or to reach the conditions favourable for effective separation. For the separation and purification of the ^{47}Sc from the activated Ti target and contaminants, a variety of separation methods, based on liquid-liquid extraction (LLX), extraction chromatography or ion exchange processes, have been investigated [42–50].

Different LLX techniques have been adopted for the separation Sc/Ti:

— Ti(IV) cupferrate salts extraction in chloroform at high HCl concentration, where scandium is poorly extracted;
— Scandium extraction by TBP according to a preferential solvation reaction with Sc;
— Multi-stage LLX using the liquid anion exchanger, trioctylamine (TOA) as an extractant;
— Multi-stage LLX using the liquid cation exchanger di-2-ethylhexylphosphoric acid (HDEHP) as an extractant.

For extraction chromatographic studies, TBP impregnated into a silica gel support or the commercial DGA (normal or branched DGA resin from Triskem) have been investigated [44, 49, 51], while for ion exchange processes AG MP 500, AG 50W-X4 cation exchange resins or combinations like anion (AG 1x8) + cation (AG50WX4) and AG MP-50 + Chelex-100 exchange resins have been studied [42–44, 49]. An innovative extraction method involving a new composite sorbent based on chitosan acrylic acid/multiwalled carbon nanotubes (CS-AA/MWCNTs) has also been recently reported. The distribution behaviour of Sc(III) and Ti(IV) ions was studied using a batch technique to optimize the separation process that was subsequently applied to a column chromatographic technique. The chromatographic column of CS-AA/MWCNTs was successfully used for the separation of ^{47}Sc from natural titanium target. The ^{47}Sc eluted fractions were of high chemical, radiochemical and radionuclidic purity [52].

4.4. RECOVERY OF TARGET MATERIAL IN PRODUCTION OF ^{47}Sc

As discussed, production routes for ^{47}Sc use either calcium or titanium targets, typically enriched for producing the desired radioisotope. Due to the high cost of enriched material, a recycling process of the target is required in most cases. However, the choice of method used in the recovery process is related to the form of the initial target material, and in particular, to the mass and the enrichment of the target.

There is a limited amount of published data on this topic. Several publications report the use of calcium carbonate targets (natural or enriched in ^{44}Ca) for production of ^{44}Sc in cyclotrons. One of the early works by Krajewski et al. reported the use of chelating resin Chelex 100 for separation of ^{44}Sc and target recycling efficiency of only 60% [38]. In work by Alliot et al., using a bicarbonate/methanol mixture, the rate of solvent evaporation was increased and the solubility of calcium carbonate was lowered [53, 54]. Recovery yield of enriched calcium of $90 \pm 2\%$ when starting with $CaCO_3$ material in the HCl solutions was obtained from the extraction process. The solution was then loaded on a pre-conditioned AG1×8 column to retain all metallic impurities (Cu, Co, Fe, etc.) and enriched ^{44}Ca was recovered in 9M HCl. This solution was evaporated to dryness, dissolved in a mixture of bicarbonate buffer (pH10.33)/methanol, filtered and the residue dried in an oven at 105°C to remove water and methanol. The recycled targets were irradiated, and no significant difference of production yield was observed (Alliot et al. [53]). The improved recovery of enriched calcium reached 98% of the initial enriched material, significantly reducing the operational costs, was reported by Van der Muelen et al. who collected effluents from the DGA column and reported enriched calcium recycling by a simple and fast precipitation method [55].

Within the CRP, at Polatom, the target material containing enriched ^{46}Ca was recovered from collected effluents via precipitation of calcium carbonate. Ammonium carbonate was added to the solutions collected after ^{47}Sc separation, until the bubbles of CO_2 disappeared. Solutions collected after scandium precipitation were acidified by adding 1 mL of 11M HCl allowing $Ca(OH)_2$ dissolution [33]. After 48 h the suspensions were centrifuged, rinsed and the precipitates were dried at 120°C for 24 h and stored for further use. The solutions were aliquoted for radiometric analysis (sampled before $CaCO_3$ precipitation and from solution after centrifugation). Gamma spectrometry with HPGe detector and liquid scintillation counting were performed. The recovery yield of ^{46}Ca was determined based on ^{45}Ca content in solutions before and after the precipitation of $CaCO_3$. Calcium-45 radioisotope was produced in a nuclear reactor from ^{44}Ca isotope present in the target material. It is a pure β^- emitter ($E_{\beta max} = 258$ keV); for this reason, measurement of its radioactivity in the presence of other radionuclides that emit higher energy β particles (such as ^{47}Ca and ^{47}Sc) is difficult. Due to the long half-life of ^{45}Ca ($T_{1/2} = 63$ d), the measurement of its radioactivity was possible after decay of the short-lived β emitters. The recovery yield of ^{46}Ca was found to be 95.8 % to 97.0% regardless of the method used for the ^{47}Sc separation process. The ^{45}Ca (in tens of MBq activities) was present in all solutions before the precipitation of [^{46}Ca]$CaCO_3$. Plans are underway to use the recovered target material for irradiation in the Maria reactor in order to confirm if its chemical purity is suitable for production of ^{47}Sc with satisfactory radionuclidic purity.

The recovery of titanium from its acidic solutions has been considered using methods reported in metallurgic industry, either using HF and HNO_3 or by producing nano sized titanium dioxide [56]. When using TiO_2 as a starting material, a recycling process has been reported by Loveless et al. [57]. The HCl solution and HNO_3 obtained from the extraction processes were collected and a solution of NH_4OH at pH 8 was added to lead to TiO_2 precipitation. The precipitate was then heated at 400°C for 4 h. When needed, the enriched titanium oxide could be reduced with calcium or calcium hydride, resulting in titanium pellets with low impurity content [58].

4.5. QUALITY CONTROL OF ^{47}Sc

The expected final form of the radionuclide prepared within the CRP, regardless of the production method, is the form of solution for radiolabelling. The European Pharmacopeia (Ph. Eur.) general monograph on radiopharmaceutical preparations (0125) can serve as a reference to establish quality specifications for the final solution of ^{47}Sc. With this general goal in mind, investigators have been developing various quality control methods. One should bear in mind that the Ph. Eur. monographs on ^{177}Lu solution for radiolabelling, 07/2017:2798, and ^{90}Y chloride solution for radiolabelling, 04/2019:2803, can provide a useful starting point as well.

An example list of tested parameters and the corresponding methods are briefly summarized below.

4.5.1. Characteristics:

(a) Appearance: clear, colourless solution;
(b) Half-life and decay characteristics of ^{47}Sc: $T_{1/2} = 3.35$ d, $E\beta^-_{mean} = 162$ keV, $E\gamma = 0.159$ MeV.

4.5.2. Identification:

(a) Gamma ray spectrometry. The most abundant γ photon of ^{47}Sc has an energy of 0.159 MeV;
(b) pH< 2.0, using a pH indicator strip.

4.5.3. Tests:

(a) Radionuclide purity: the Ph. Eur. recommended limit is minimum 99.9% of the total radioactivity. The expected radionuclide contaminants are ^{46}Sc($T_{1/2} = 83.8$ d) and ^{48}Sc($T_{1/2} = 43.7$ h). Although their presence has been reported by participants, the limits for individual radionuclide impurities were not yet determined;
(b) Chemical purity: the ions of Cu, Fe, Zc and Pb and the traces of target material such as Ca or Ti. Since DOTA is the most common chelator used for labelling with ^{47}Sc, it can be assumed that the content of chemical impurities such as copper, iron, zinc and lead ions may have impact on ^{47}Sc quality. The content of chemical impurities may vary depending on the processing method and purity of reagents. The methods used for determination of chemical contaminants presented by the participants included determination of Ti using ICP–mass spectrometry (with consideration of isotopic abundance) or determination of metallic impurities by ICP atomic emission spectrometry. These instrumental techniques can be employed to establish the chemical impurity acceptance levels. Routine use of such methods is however a challenge due lack of such sophisticated/high cost equipment at most facilities and challenges in access to third party laboratories which will accept radioactive samples. Alternative tests might be of consideration (e.g. indirectly demonstrating an acceptable metallic purity profile by showing that it is possible to incorporate into a chelator such as DOTA, with a minimum molar activity);
(c) Radiochemical purity: in the Ph. Eur. monographs for ^{177}Lu and ^{90}Y solutions for radiolabelling, for the assessment of radiochemical purity via thin layer chromatography (TLC) system, the method recommends using complexes of these radiometals with pentetic acid as reference. In the CRP it was recommended to test the radiochemical purity of obtained ^{47}Sc when used for radiolabelling of selected common chelators such as DOTA, DTPA (diethylenetriaminepentaacetic acid) or EDTA, or peptide conjugates such as DOTATATE or DOTA bombesin, with further TLC development to assess the radiochemical purity of ^{47}Sc labelled compound. Usually, the radiochemical purity should be not less than 98% to 99% to confirm the quality of ^{47}Sc. This approach can serve also as the indirect confirmation of ^{47}Sc

chemical purity suitability for radiolabelling. In addition, the experiments can be designed to check the apparent molar activity of the isolated ^{47}Sc solutions. Such tests provide very useful information during the process development, especially when instrumental methods for determination of chemical purity are not available on-site;

(d) Bacterial endotoxins: less than 175 IU/V, V being the maximum volume to be used for the preparation of a single patient dose, if intended for use in the manufacture of parenteral preparations without a further appropriate procedure for the removal of bacterial endotoxins.

4.6. RADIOLABELLING AND APPLICATIONS WITH ^{47}Sc

The commonly used chelator for radiolabelling biomolecules with ^{47}Sc is DOTA. For radiolabelling with [^{47}Sc]ScCl$_3$, similar radiolabelling conditions can be applied reported for ^{67}Cu. Radiolabelling efficiency can be measured by using TLC and/or high performance liquid chromatography (HPLC) analysis to determine the radiochemical purity of the labelled product.

4.6.1. Sample radiolabelling procedure for ^{47}Sc

— 25 μg to 50 μg of DOTA conjugated peptide (1 mg/mL stock solution);
— 0.1M NH$_4$OAc (pH4–5);
— 50 to 100 μL of gentisic acid or ascorbic acid (50 mg/mL in water);
— [^{47}Sc]ScCl$_3$ (~2 mCi);
— Heating at 90°C for 20 to 30 min.

Quality Control: Determination of the amount of unlabelled ^{47}Sc by radio-TLC and/or radio-HPLC analysis to measure the radiolabelling efficiency. Usual recommended radiochemical purity of higher than 98–99% is desired to confirm the quality of ^{47}Sc labelled radiopharmaceutical.

4.6.2. Sample HPLC purification and analysis

HPLC analysis and purification of the bioconjugates were performed on a Shimadzu HPLC system using a C18 reversed phase column (5 μm, 3.9×150 mm), a UV-VIS detector set at 220 nm, a flow count γ radioactivity detection system and a suitable HPLC chromatogram analysis program. The HPLC used a gradient system of 0.1% (v/v) trifluoro acetic acid in water (solvent A) and 0.1% (v/v) trifluoro acetic acid in acetonitrile (solvent B) at a flow rate of 0.9 mL/min. The HPLC gradient system began with a solvent composition of 95% A and 5% B from 0 min to 2.5 min followed by a linear gradient of 95% A and 5% B to 5% A and 95% B over 30 min. The gradient remained at this level for 3 min before switching back to 95% A and 5% B for another 7 min. Radiochemical purity was estimated by evaluating radioactivity peaks eluted for each radiopeptide from the reserve phase HPLC column and calculating the area under the peak or region of interest. For each peptide, the major peak was isolated, and the organic solvent was evaporated under a gentle stream of nitrogen gas. The HPLC purified compounds were reconstituted in sterile saline for in vitro and in vivo studies. The stability of radiolabelled compounds was evaluated in the presence of a competitor for the Cu ions, such as DTPA. For this purpose, up to 1 000 times molar excess of DTPA was added to the radiolabelled conjugate before incubating at 37°C for up to 24 h. Samples of this mixture were removed at different time points and analysed by radio-HPLC as described above.

4.6.3. Preclinical evaluation (experimental procedures)

4.6.3.1.Octanol-saline partition coefficient

To determine the lipophilicity, each HPLC-purified radiolabelled compounds (100 µL) was added to a test tube each containing 1 mL of *n*-octanol and 1 mL of saline. The tube was vortexed mixed for 1 min. After partial separation of the phases by gravity for another 15 min, 0.5 mL of each phase was transferred to separate tubes and centrifuged at 5 000 xg for 5 min. Duplicate 100 µL aliquots of each phase were taken for radioactivity measurement using a γ counter and the partition coefficient was determined by the function: Partition coefficient $=\text{Log}_{10}$ (radioactivity in octanol layer/radioactivity in aqueous layers).

4.6.3.2. In vitro stability in plasma and in MDA-MB-23 or PC-3 cells

Each radiolabelled peptide (100 µL, ~200 µCi) was incubated with human plasma (500 µL) in duplicate at 37°C for up to 4 h. For ^{47}Sc labelled peptides, incubation time was extended up to 72 h. Following incubation at different time points, the plasma proteins were precipitated with a mixture of CH3CN/EtOH(1:1v/v) and the samples were centrifuged at 5 000 xg for 5 min. The supernatant layer was filtered through a 0.2 µm pore filter and was analysed by radio-HPLC under the conditions described above in order to determine the in vitro metabolic stability of the radiopeptides. The stability in the cell cultures were examined by incubating each radiolabelled peptide (50 µL, 100 µCi) with an MDA-MB-231 or PC-3 cell suspension (~300 000 cells in 0.3 mL) in phosphate buffered saline at 37°C for 2 h. The mixtures were then centrifuged, and the supernatant layers was analysed by HPLC (as described above) to determine the stability of radiolabelled peptide conjugates in the cell culture.

4.6.3.3. Cell culture preparation

Human breast cancer cell lines: MDA-MB-231, MCF-7, T47-D and prostate PC-3 cancer cell lines were grown as mono layers at 37°C in a humidified atmosphere in RPMI-1640 culture media with 10% fetal bovine serum in tissue culture flasks. 24 h prior to conducting the binding assay, the media was replaced with RPMI-1640/10% fetal bovine serum. The cells were grown to confluency and harvested by trypsinization. After centrifugation, $\sim 5 \times 10^6$ cells were suspended in 5 mL media for binding assays.

4.6.3.4. In vitro cell binding and internalization

The cell binding and subsequent internalization into various breast cancer cell lines of radiolabelled conjugates were performed as follows. Approximately 300 000 cells (in 300 µL phosphate buffered saline) were incubated with various amounts of radioligands (prepared from the serial dilutions of HPLC-purified radiopeptides) in duplicate for 60 min at room temperature. Incubation was terminated by dilution with cold saline (300 µL) and the cells were pelleted by centrifugation. The cell-pellets were rapidly washed with cold saline to remove any unbound peptide and centrifuged to collect supernatants. Radioactivity in the cell-pellet and the washings were measured in a γ counter. Non-specific binding was determined in the presence of approximately 100-fold excess of unlabelled peptide. Specific binding was calculated by subtracting the non-specifically bound radioactivity from that of the total binding. The binding data was analysed (to estimate respective binding affinities) by a non-linear regression analysis program, using a one site binding equation. Thereafter, the cell pellets were incubated again with 300 µL of acidic buffer (0.02 M sodium acetate in saline, pH5.0) at 37°C

for 5 min to allow cellular internalization of the surface bound radioligand. After incubation, cells were separated by centrifugation and washed with cold acidic buffer. The amount of cell surface bound (acid wash) and intracellular radioactivity (remainder) were determined by measuring the radioactivity of the supernatants and the cell-pellets, respectively, in a γ counter.

4.6.3.5. In vivo animal biodistribution

Prior approval was obtained from the institutional Animal Safety and Care Committee for the use of animals. Animal studies were conducted according to the international regulations governing the safe and proper use of laboratory animals. In vivo biodistribution studies were performed on healthy Balb/c mice (body mass 18g to 25g) and nude mice implanted with either MDA-MB-231 breast or PC-3 prostate cancer cells. The HPLC purified radioligand (100 µL, ~20 µCi, total peptide dose ranged from 1 to 5 µg) was injected intravenously via the lateral tail vein and the animals (n = 3 to 5 animals per time point) were sacrificed by neck dislocation at 1 h, 4 h and 24 h post-injection (p.i.).The blood and urine were immediately collected. Any urine expelled on sacrificing the animals was measured together with that remaining in the bladder. Major organs (lungs, stomach, liver, kidneys, intestines, etc.) were isolated, weighed and the radioactivity was measured in a γ counter. The percentage injected dose per gram (% injected dose/g) of tissue was calculated by counting the samples in a γ counter against the suitably diluted aliquots of the injected solution as a standard. For clearance studies, radioactivity in the urine with bladder and intestines with contents is reported as the percentage of the injected dose (% injected dose). The biodistribution data was analysed by using a custom designed computer program on Quattro Pro 6.0 spread sheet (NovellInc., USA). In vivo receptor blocking studies were also carried out where excess unlabelled peptide (~100 µg) was injected intramuscularly in mice for in vivo saturation of peptide receptors, 20 min prior to the administration of radiopeptide. In vivo biodistribution were conducted at 1 h p.i. as described above.

4.6.3.6. In vivo tumour targeting

Mouse tumour models have proven to be important tools for furthering our understanding of human cancer. Human xenografts mouse models with receptor positive cancer cell lines (BN, HER2/neu, MUC-1 and PSA-positive cell lines), were used for in vivo tumour targeting studies. For the induction of tumour xenografts, approximately 1×10^7 cancer cells suspension (in 200 µL sterile saline) were injected subcutaneously per mouse. After 4 to 6 weeks of post-inoculation the tumours achieved adequate growth (~0.3–0.7 g solid palpable mass) and biodistribution and tumour uptake studies were performed at 1 h, 4 h and 24 h p.i. The amount of radioactivity in the tumours and other major organs (i.e. stomach, pancreas, lungs, liver, kidneys, etc.) was determined by γ counting as described above for Balb/c mice.

5. DISCUSSION AND FUTURE DIRECTIONS

Numerous routes have been described above for the production of ^{67}Cu, ^{186}Re, and ^{47}Sc, including ^{67}Cu production from nickel or zinc targets, ^{186}Re production from tungsten targets, ^{47}Sc from calcium, titanium, or vanadium targets. Additionally, for the case of ^{47}Sc, both a direct production route and the $^{47}Ca \rightarrow ^{47}Sc$ generator like approach may be practical. With regards to which route should be chosen to produce one of these nuclides there is no one answer. As a primary consideration, a site will be constrained by the availability of projectile (e.g. n, p, α, γ, etc.) of a suitable energy range. There are many additional practical considerations when selecting a production route, several of which are described below.

The production yields for these different reactions schemes vary significantly, and some routes may result in activity yields which might be too low for production of clinically relevant quantities. Nevertheless, access to low yielding routes may be of great benefit to those sites developing targetry and chemical separation methods, sites looking at novel radiochemistry/radiolabelling methods and/or tracers or chelators, or perhaps sites wishing to perform in vitro or pre-clinical studies.

It is also important to consider any radionuclidic impurities which are co-produced during irradiation, both for different reaction schemes and/or for different irradiation energies within a given production route. While chemical purification can be used to separate radionuclidic impurities of different elemental form than the desired product, it is not possible to separate radioisotopic impurities (e.g. ^{64}Cu from ^{67}Cu, ^{46}Sc from ^{47}Sc, or ^{184}Re from ^{186}Re). Albeit based largely on a nuclear model codes, and thus must be experimentally confirmed, one may wish to refer to the IAEA Medical Isotope Brower tool as a first prediction of possible co-produced nuclides. Understanding the additional clinical radiation dose arising from such impurities is important and may involve dosimetry calculations and engagement with clinicians for input on acceptable specifications.

An additional consideration is the question of cost. While a site might choose to use natural abundance materials for initial development efforts, nearly all the proposed methods ultimately benefit from, if not require, enriched target materials for producing a high quality product. Taking ^{46}Ca with a natural isotopic abundance of 0.004% as an example, proposed target materials may be of very low natural abundance. The cost of such enriched materials may potentially be prohibitive and, in some cases, may not be commercially available to the desired enrichment levels. While there may be significant cost associated with production of the larger scale production of radionuclides of this CRP, one should similarly consider that the cost of procuring other therapy nuclides beyond those described in this CRP (e.g. ^{177}Lu) is generally not negligible.

Considering other radiometal therapy nuclides such as ^{177}Lu, it is important to highlight that copper and scandium have a unique property of having both β^+ emitting isotopes such as ^{60,61,64}Cu or ^{43,44}Sc and β^- emitting isotopes of ^{67}Cu and ^{47}Sc, thereby allowing for a true theranostic pairing of quantitative PET with therapy. While non-matched pairs are common and have been implemented in clinical practice (e.g. ^{68}Ga/^{177}Lu), it should be cautioned that radiolabelling of the same molecule with two different elements can, at times (but not necessarily), result in significantly different kinetics/biodistributions. In other words, identical biodistributions should not be taken for granted for non-matched pairs.

Regardless of which nuclide a site wishes to work with and which production route is selected, for clinical production, it is important to establish quality control methods, have a quality assurance program, and consider ease/suitability of production methods to ultimate labelling of a radiopharmaceutical in accordance with good manufacturing practice.

While not a significant focus over the course of this CRP, other underdeveloped production routes such as photonuclear activation might lead to widespread availability of these promising radionuclides. In particular, recent works have illustrated the utility of this approach for the production of ^{67}Cu and ^{47}Sc [43, 59–62]. While high intensity electron accelerators are less widely available than proton or deuteron accelerators, recent studies in this area have illustrated that the production of large scale quantities (GBq) are possible if challenges with heat dissipation and chemistry for the large amounts of required target material can be overcome.

REFERENCES

[1]   MASTREN, T., et al., Cyclotron production of high-specific activity ^{55}Co and in vivo evaluation of the stability of ^{55}Co metal-chelate-peptide complexes, Mol. Imaging **14** (2015) 526.

[2]   JALILIAN, A.R. et al., IAEA activities on ^{67}Cu, ^{186}Re, ^{47}Sc Theranostic radionuclides and Radiopharmaceuticals, Curr Radiopharm (2020).

[3]   KONING, A.J., et al., TENDL: Complete nuclear data library for innovative nuclear science and technology, Spec. Issue Nucl. React. Data **155** (2019) 1.

[4]   ENGLE, J.W., et al., Recommended nuclear data for the production of selected therapeutic radionuclides, Spec. Issue Nucl. React. Data **155** (2019) 56.

[5]   PUPILLO, G., et al., New production cross sections for the theranostic radionuclide ^{67}Cu, Nucl. Instrum. Methods Phys. Res. Sect. B Beam Interact. Mater. At. **415** (2018) 41.

[6]   The Radiochemistry of Copper, The National Academies Press, Washington, DC (1961).

[7]   STRELOW, F.W.E., VICTOR, A.H., VAN ZYL, C.R., ELOFF, Cynthia., Distribution coefficients and cation exchange behavior of elements in hydrochloric acid-acetone, Anal. Chem. **43** (1971) 870.

[8]   OHYA, T., et al., Small-scale production of ^{67}Cu for a preclinical study via the ^{64}Ni(α, p)^{67}Cu channel, Nucl. Med. Biol. **59** (2018) 56.

[9]   OHYA, T., et al., Efficient preparation of high-quality ^{64}Cu for routine use, Nucl. Med. Biol. **43** (2016) 685.

[10]   MCCARTHY, D.W., et al., Efficient production of high specific activity ^{64}Cu using a biomedical cyclotron, Nucl. Med. Biol. **24** 1 (1997) 35.

[11]   LE, V.S., et al., Alternative method for ^{64}Cu radioisotope production, Appl. Radiat. Isot. Data Instrum. Methods Use Agric. Ind. Med. **67** (2009) 1324.

[12]   AL RAYYES, A.H., AILOUTI, Y., Production and quality control of ^{64}Cu from high current Ni target, World J. Nucl. Sci. Technol. **3** (2013) 72.

[13]   MATTERS, D.A. et al., Investigation of ^{186}Re via radiative thermal-neutron capture on ^{185}Re, Phys. Rev. **93** (2016) 054319.

[14]   DRUZHININ, A., LBOV, A., BILIBIN, L., Cross sections of fast-neutron reactions (n, gamma) and (n, 2n) for Re isotopes, Sov. J. Nucl. Phys. USSR **5** (1967) 13.

[15]   HUSSAIN, M., et al., Evaluation of charged particle induced reaction cross section data for production of the important therapeutic radionuclide ^{186}Re, Radiochim. Acta **98** (2010) 385.

[16]   KHANDAKER, M.U., et al., Study of deuteron-induced nuclear reactions on natural tungsten for the production of theranostic ^{186}Re via AVF cyclotron up to ^{38}MeV, Nucl. Instrum. Methods Phys. Res. Sect. B Beam Interact. Mater. At. **403** (2017) 51.

[17]   SCOTT, N.E., COBBLE, J.W., DALY, P.J., A comparison of reactions induced by medium-energy ^{3}He and ^{4}He ions in heavy target nuclei, Nucl. Phys. A **119** (1968) 131.

[18]   ENQVIST, T., et al., Isotopic yields and kinetic energies of primary residues in 1 A GeV ^{208}Pb+p reactions, Nucl. Phys. A **686** (2001) 481.

[19]   REJMUND, F., et al., Measurement of isotopic cross sections of spallation residues in 800 A MeV ^{197}Au+p collisions, Nucl. Phys. A **683** (2001) 540.

[20]   GUERTIN, A., DUCHEMIN, C., HADDAD, F., MICHEL, N., MÉTIVIER, V., Measurements of ^{186}Re production cross section induced by deuterons on ^{nat}W target at ARRONAX facility, Nucl. Med. Biol. **41 Suppl** (2014) e16.

[21]   BONARDI, M.L., GROPPI, F., MANENTI, S., PERSICO, E., GINI, L., Production study of high specific activity NCA ^{186g}Re by proton and deuteron cyclotron irradiation, Appl. Radiat. Isot. Data Instrum. Methods Use Agric. Ind. Med. **68** (2010) 1595.

[22]   LAPI, S., et al., Production cross-sections of $^{181-186}$Re isotopes from proton bombardment of natural tungsten, Appl. Radiat. Isot. Data Instrum. Methods Use Agric. Ind. Med. **65** (2007) 345.

[23]   CHAKRAVARTY, R., et al., A facile method for electrochemical separation of $^{181-186}$Re from

proton irradiated natural tungsten oxide target, Appl. Radiat. Isot. Data Instrum. Methods Use Agric. Ind. Med. **154** (2019) 108885.

[24]   MOUSTAPHA, M.E., et al., Preparation of cyclotron-produced [186]Re and comparison with reactor-produced [186]Re and generator-produced [188]Re for the labeling of bombesin, Nucl. Med. Biol. **33** (2006) 81.

[25]   GOTT, M.D. et al., Accelerator-based production of the [99m]Tc-[186]Re diagnostic-therapeutic pair using metal disulfide targets (MoS2, WS2, OsS2), Appl. Radiat. Isot. Data Instrum. Methods Use Agric. Ind. Med. **114** (2016) 159.

[26]   ISHIOKA, Noriko.S., et al., Excitation functions of rhenium isotopes on the [nat]W(d, xn) reactions and production of no-carrier-added [186]Re, J. Nucl. Sci. Technol. **39** (2002) 1334.

[27]   ALI, S.K., KHANDAKER, M.U., KASSIM, H.A., Evaluation of production cross-sections for [186]Re theranostic radionuclide via charged-particle induced reactions on Tungsten, Appl. Radiat. Isot. **135** (2018) 239.

[28]   NATIONAL NUCLEAR DATA CENTER, NuDat 2.8 Interactive Chart of Nuclides, https://www.nndc.bnl.gov/nudat2/

[29]   MISIAK, R., et al., [47]Sc production development by cyclotron irradiation of [48]Ca, J. Radioanal. Nucl. Chem. **313** (2017) 429.

[30]   MINEGISHI, K., et al., Production of scandium-43 and-47 from a powdery calcium oxide target via the nat/[44]Ca (α, x)-channel, Appl. Radiat. Isot. **116** (2016) 8.

[31]   PUPILLO, G., et al., Production of [47]Sc with natural vanadium targets: Results of the PASTA project, J. Radioanal. Nucl. Chem. **322** (2019) 1711.

[32]   GIZAWY, M.A., MOHAMED, N.M.A., AYDIA, M.I., SOLIMAN, M.A., SHAMSEL-DIN, H.A., Feasibility study on production of Sc-47 from neutron irradiated Ca target for cancer theranostics applications, Radiochim. Acta **108** (2020) 207.

[33]   PAWLAK, D., et al., Comparison of separation methods for [47]Ca/[47]Sc radionuclide generator, Appl. Radiat. Isot. Data Instrum. Methods Use Agric. Ind. Med. **151** (2019) 140.

[34]   CHAKRAVARTY, R., CHAKRABORTY, S., RAM, R., DASH, A., An electroamalgamation approach to separate [47]Sc from neutron-activated [46]Ca target for use in cancer theranostics, Sep. Sci. Technol. **52** (2017) 2363.

[35]   DOMNANICH, K.A., et al., [47]Sc as useful β–emitter for the radiotheragnostic paradigm: A comparative study of feasible production routes, EJNMMI Radiopharm. Chem. **2** (2017) 1.

[36]   SIWOWSKA, K., et al., Therapeutic potential of [47]Sc in comparison to ^{177}Lu and [90]Y: Preclinical investigations, Pharmaceutics **11** (2019).

[37]   WALCZAK, R. et al., Cyclotron production of [43]Sc for PET imaging, EJNMMI Phys. **2** (2015) 33.

[38]   KRAJEWSKI, S., et al., Cyclotron production of [44]Sc for clinical application, Radiochim. Acta **101** (2013) 333.

[39]   VALDOVINOS, H.F., et al., Separation of cyclotron-produced [44]Sc from a natural calcium target using a dipentyl pentylphosphonate functionalized extraction resin, Appl. Radiat. Isot. **95** (2015) 23.

[40]   MÜLLER, C., et al., Promises of cyclotron-produced [44]Sc as a diagnostic match for trivalent β−emitters: In vitro and in vivo study of a [44]Sc-DOTA-folate conjugate, J. Nucl. Med. **54** (2013) 2168.

[41]   SEVERIN, G.W., et al., [44g]Sc from metal calcium targets for PET, AIP Conference Proceedings, Vol. 1509, American Institute of Physics (2012) 125–128.

[42]   BARTOS, B., MAJKOWSKA, A., KASPEREK, A., KRAJEWSKI, S., BILEWICZ, A., New separation method of no-carrier-added [47]Sc from titanium targets, Radiochim. Acta **100** (2012) 457.

[43]   LOVELESS, C.S., et al., Photonuclear production, chemistry, and in vitro evaluation of the theranostic radionuclide [47]Sc, EJNMMI Res. **9** (2019) 42.

[44]   PIETRELLI, L., MAUSNER, L.F., KOLSKY, K.L., Separation of carrier-free [47]Sc from

titanium targets, J. Radioanal. Nucl. Chem. **157** (1992) 335.

[45] ALY, H.F., EL-HAGGAN, M.A., Production of carrier-free scandium radioisotopes from a neutron-irradiated potassium titanium oxalate target, Microchim. Acta **59** (1971) 4.

[46] DAS, M.K., SARKAR, B.R., RAMAMOORTHY, N., Yields of some Radioisotopes formed in α-particle induced reactions on titanium and recovery of scandium radionuclides, Radiochim. Acta **50** (1990) 135.

[47] DAS, N., BANERJEE, S., LAHIRI, S., Sequential separation of carrier free ^{47}Sc, ^{48}V and $^{48, 49, 51}$Cr from α-particle activated titanium with TOA, Radiochim. Acta **69** (1995) 61.

[48] LAHIRI, S., BANERJEE, S., DAS, N.R., LLX separation of carrier-free ^{47}Sc, ^{48}V and ^{48,49,51}Cr produced in α-particle activated titanium with HDEHP, Appl. Radiat. Isot. **47** (1996) 1.

[49] KOLSKY, K.L., JOSHI, V., MAUSNER, L.F., SRIVASTAVA, S.C., Radiochemical purification of no-carrier-added scandium-47 for radioimmunotherapy, Appl. Radiat. Isot. Data Instrum. Methods Use Agric. Ind. Med. **49** (1998) 1541.

[50] BOKHARI, T.H., MUSHTAQ, A., KHAN, I.U., Separation of no-carrier-added radioactive scandium from neutron irradiated titanium, J. Radioanal. Nucl. Chem. **283** (2010) 389.

[51] BOSCHI, A., MARTINI, P., COSTA, V., PAGNONI, A., UCCELLI, L., Interdisciplinary tasks in the cyclotron production of radiometals for medical applications. The case of ^{47}Sc as example, Mol. Basel Switz. **24** (2019).

[52] GIZAWY, M.A., et al., Synthesis of chitosan-acrylic acid/multiwalled carbon nanotubes composite for theranostic ^{47}Sc separation from neutron irradiated titanium target, Int. J. Biol. Macromol. **163** (2020) 79.

[53] ALLIOT, C., KERDJOUDJ, R., MICHEL, N., HADDAD, F., HUCLIER-MARKAI, S., Cyclotron production of high purity ^{44m,44}Sc with deuterons from ^{44}CaCO3 targets, Nucl. Med. Biol. **42** (2015) 524.

[54] KAN, A.T., FU, G., TOMSON, M.B., Effect of methanol on carbonate equilibrium and calcite solubility in a gas/methanol/water/salt mixed system, Langmuir **18** (2002) 9713.

[55] VAN DER MEULEN, N.P. et al., Cyclotron production of ^{44}Sc: From bench to bedside, Nucl. Med. Biol. **42** (2015) 745.

[56] DEILAMI-NEZHAD, L., MOGHADDAM-BANAEM, L., SADEGHI, M., ASGARI, M., Production and purification of scandium-47: A potential radioisotope for cancer theranostics, Appl. Radiat. Isot. Data Instrum. Methods Use Agric. Ind. Med. **118** (2016) 124.

[57] LOVELESS, C., BLANCO, J., BRACCINI, S., LAPI, S., Evaluation of cyclotron produced ^{43,44,47}Sc from titanium (0) and titanium dioxide, J. Label. Compd. Radiopharm. (2019) 569.

[58] LOMMEL, B., et al., Reduction of isotopically enriched ^{50}Ti-dioxide for the production of high-intensity heavy-ion beam, J. Radioanal. Nucl. Chem. **299** (2014) 977.

[59] HABS, D., KÖSTER, U., Production of medical radioisotopes with high specific activity in photonuclear reactions with γ-beams of high intensity and large brilliance, Appl. Phys. B **103** (2011) 501.

[60] ROTSCH, D.A. et al., Electron linear accelerator production and purification of scandium-47 from titanium dioxide targets, Appl. Radiat. Isot. **131** (2018) 77.

[61] HOWARD, S., STAROVOITOVA, V.N., Target optimization for the photonuclear production of radioisotopes, Appl. Radiat. Isot. Data Instrum. Methods Use Agric. Ind. Med. **96** (2015) 162.

[62] SMITH, N.A., BOWERS, D.L., EHST, D.A., The production, separation, and use of ^{67}Cu for radioimmunotherapy: a review, Appl. Radiat. Isot. **70** 10 (2012) 2377.

ABBREVIATIONS

CRP   coordinated research project
DOTA   1,4,710-tetraazacyclododecane-1,4,7,10-tetraacetic acid
DTPA   diethylenetriaminepentaacetic acid
EOB   end of bombardment
ICP   inductively coupled plasma
HPLC   high performance liquid chromatography
LLX   liquid-liquid extraction
NCA   no carrier added
PET   positron emission tomography
Ph. Eur.   european pharmacopeia
TLC   thin layer chromatography

CONTRIBUTORS TO DRAFTING AND REVIEW

Aboudzadeh-Rovais M.	Nuclear Science and technology Research Institute, Iran
Alliot, C.	GIP ARRONAX, France
Al Rayyes, A.	Atomic Energy Commission of Syria, Syria
Bilewicz, A.	Institute of Nuclear Chemistry and Technology, Poland
Chakraborty, S.	Bhabha Atomic Research Centre, India
Gagnon, K.	GE Healthcare, Sweden
Gizawy, M.	Egyptian Atomic Energy Authority, Egypt
Jalilian A.	International Atomic Energy Agency
Khandaker, M.U.	University of Malaya, Malaysia
Lapi, S.E.	University of Alabama, USA
Mikołajczak, R.	National Centre for Nuclear Research, Poland
Nagatsu, K.	National Institute of Radiological Sciences, Japan
Osso, Jr. J.	International Atomic Energy Agency, Austria
Okarvi, S.	King Faisal Specialist Hospital and Research Centre, Saudi Arabia
Park, J.H.	Korea Atomic Energy Research Institute (KAERI), Korea
Pupillo, G.	Istituto Nazionale di Fisica Nucleare, LNL, Italy
Takacs, S.	Hungarian Academy of Sciences, Hungary

This Tec-Doc was an outcome of the IAEA Coordinated Research Project, titled *"Therapeutic Radiopharmaceuticals Labelled with New Emerging Radionuclides (^{67}Cu, ^{186}Re, ^{47}Sc) F22053"*

ORDERING LOCALLY

IAEA priced publications may be purchased from the sources listed below or from major local booksellers.

Orders for unpriced publications should be made directly to the IAEA. The contact details are given at the end of this list.

NORTH AMERICA

Bernan / Rowman & Littlefield

15250 NBN Way, Blue Ridge Summit, PA 17214, USA
Telephone: +1 800 462 6420 • Fax: +1 800 338 4550

Email: orders@rowman.com • Web site: www.rowman.com/bernan

REST OF WORLD

Please contact your preferred local supplier, or our lead distributor:

Eurospan Group

Gray's Inn House
127 Clerkenwell Road
London EC1R 5DB
United Kingdom

Trade orders and enquiries:

Telephone: +44 (0)176 760 4972 • Fax: +44 (0)176 760 1640
Email: eurospan@turpin-distribution.com

Individual orders:

www.eurospanbookstore.com/iaea

For further information:

Telephone: +44 (0)207 240 0856 • Fax: +44 (0)207 379 0609
Email: info@eurospangroup.com • Web site: www.eurospangroup.com

Orders for both priced and unpriced publications may be addressed directly to:

Marketing and Sales Unit
International Atomic Energy Agency
Vienna International Centre, PO Box 100, 1400 Vienna, Austria
Telephone: +43 1 2600 22529 or 22530 • Fax: +43 1 26007 22529
Email: sales.publications@iaea.org • Web site: www.iaea.org/publications

21-00130E

International Atomic Energy Agency
Vienna